THE JOURNAL OF BIOLOGICAL CHEMISTRY VOL. 291, NO. 4, pp. 1933–1947, January 22, 2016

Nuclear Factor of Activated T Cells-dependent Down-regulation of the Transcription Factor Glioma-associated Protein 1 (GLI1) Underlies the Growth Inhibitory Properties of Arachidonic Acid*

Received for publication, September 14, 2015, and in revised form, November 18, 2015 Published, JBC Papers in Press, November 24, 2015, DOI 10.1074/jbc.M115.691972

Andrea Comba[‡§1], Luciana L. Almada[‡], Ezequiel J. Tolosa[‡], Eriko Iguchi[‡], David L. Marks[‡], Marianela Vara Messler[§], Renata Silva[§], Maite G. Fernandez-Barrena[‡], Elisa Enriquez-Hesles[‡], Anne L. Vrabel[‡], Bruno Botta[¶], Lucia Di Marcotulio[‖], Volker Ellenrieder[**], Aldo R. Eynard[§], Maria E. Pasqualini[§], and Martin E. Fernandez-Zapico[‡2]

From the [‡]Schulze Center for Novel Therapeutics, Division of Oncology Research, Mayo Clinic, Rochester, Minnesota 55905, [§]Instituto de Investigaciones en Ciencias de la Salud, Consejo Nacional de Investigaciones Científicas y Técnicas and Facultad de Ciencias Médicas-Universidad Nacional de Córdoba, Ciudad Universitaria, 5000 Córdoba, Argentina, [¶]Dipartimento di Chimica e Tecnologie del Farmaco, Sapienza University, Center for Life Nano Science at Sapienza, Istituto Italiano di Tecnologia, 00161 Rome, Italy, [‖]Department of Molecular Medicine, Sapienza University, Pasteur Institute/Cenci-Bolognetti Foundation, 00161 Rome, Italy, and [**]Gastroenterology and Gastrointestinal Oncology, University Medical Center Göttingen, 37075 Göttingen, Germany

Numerous reports have demonstrated a tumor inhibitory effect of polyunsaturated fatty acids (PUFAs). However, the molecular mechanisms modulating this phenomenon are in part poorly understood. Here, we provide evidence of a novel antitumoral mechanism of the PUFA arachidonic acid (AA). *In vivo* and *in vitro* experiments showed that AA treatment decreased tumor growth and metastasis and increased apoptosis. Molecular analysis of this effect showed significantly reduced expression of a subset of antiapoptotic proteins, including BCL2, BFL1/A1, and 4-1BB, in AA-treated cells. We demonstrated that down-regulation of the transcription factor glioma-associated protein 1 (GLI1) in AA-treated cells is the underlying mechanism controlling BCL2, BFL1/A1, and 4-1BB expression. Using luciferase reporters, chromatin immunoprecipitation, and expression studies, we found that GLI1 binds to the promoter of these antiapoptotic molecules and regulates their expression and promoter activity. We provide evidence that AA-induced apoptosis and down-regulation of antiapoptotic genes can be inhibited by overexpressing GLI1 in AA-sensitive cells. Conversely, inhibition of GLI1 mimics AA treatments, leading to decreased tumor growth, cell viability, and expression of antiapoptotic molecules. Further characterization showed that AA represses GLI1 expression by stimulating nuclear translocation of NFATc1, which then binds the *GLI1* promoter and represses its transcription. AA was shown to increase reactive oxygen species. Treatment with antioxidants impaired the AA-induced apoptosis and down-regulation of GLI1 and NFATc1 activation, indicating that NFATc1 activation and GLI1 repression require the generation of reactive oxygen species. Collectively, these results define a novel mechanism underlying AA antitumoral functions that may serve as a foundation for future PUFA-based therapeutic approaches.

Epidemiological and experimental studies have demonstrated a role for polyunsaturated fatty acids (PUFAs)[3] in different aspects of tumor development (1–3). PUFAs have been reported to have both pro- and antitumoral properties (4). In particular, the roles of dietary ω-3 and ω-6 PUFAs in cancer prevention have been explored (5, 6). Both *in vitro* and *in vivo* studies as well as clinical studies have implicated different fatty acids in tumor development and progression. Increased cellular levels of PUFAs have been shown to inhibit tumor growth (7). *In vivo* intratumoral injection of PUFAs induces tumor regression (8–10) and improves survival (11). Moreover, clinical studies have shown that intratumoral injection of PUFAs in patients with intractable gliomas improves survival and induces partial tumor regression without causing side effects (12, 13).

PUFAs can also act as cytotoxic molecules, activating different cell signaling pathways that modulate proliferation, cell death, and migration of tumor cells (14, 15). The cytotoxic effects of PUFAs have been suggested to occur in part due to alterations in reactive oxygen species, changes in cell membrane fluidity or conversion of PUFAs to highly bioactive metabolites such as prostaglandins and leukotrienes, and/or altered expression of genes that regulate apoptotic cell death (6,

* This work was supported in part by the National Institutes of Health Grants CA136526 from the NCI, P50 CA102701 through the Mayo Clinic Pancreatic Specialized Program of Research Excellence, and P30 DK84567 through the Mayo Clinic Center for Cell Signaling in Gastroenterology (to M. E. F.-Z.), Consejo Nacional de Investigaciones Científicas y Técnicas-Argentina (CONICET)-PIP 2009–2011 Grant 11220080103014 and (CONICET)-PIP 2012–2014 Grant 11220110101010 (to A. R. E.), and Secretaria de Ciencia y Tecnología de la Universidad Nacional de Córdoba-Argentina (SECYT-UNC) Grants 214/10 (to M. E. P.). The authors have declared that no conflict of interest exists. The content is solely the responsibility of the authors and does not necessarily represent the official views of the National Institutes of Health.

[1] A fellow at CONICET.

[2] To whom correspondence should be addressed. E-mail: fernandezzapico.martin@mayo.edu.

[3] The abbreviations used are: PUFA, polyunsaturated fatty acid; AA, arachidonic acid; CsA, cyclosporin A; GLI, glioma-associated protein; NAC, *N*-acetylcysteine; NFAT, nuclear factor of activated T cells; LA, linoleic acid; PA, palmitoleic acid; Q-VD-OPH, quinoline-Val-Asp-difluorophenoxymethylketone; LUC, luciferase; q-PCR, quantitative-PCR; m, mouse; h, human; CASP, caspase.

16–22). However, the molecular pathways by which PUFAs regulate cell death in cancer cells are poorly understood.

Here, using the PUFA arachidonic acid (AA) *in vitro* and *in vivo*, we define a novel mechanism underlying the tumor inhibitory function of this fatty acid. AA is a member of the ω-6 family, derived by successive elongation and desaturation from the essential fatty acid linoleic acid (LA), the major PUFA of cell membranes present at the sn-2 position of glycerophospholipids. Direct cell supplementation with AA has cytotoxic activity and decreases cell viability in different tumor cell types, including cervical, hepatic, and pancreatic (23–25). In this study, we identify *GLI1*, a known oncogenic transcription factor (26), as a target of AA signaling in cancer cells. GLI1 is a member of the GLI family of C_2H_2 zinc finger transcription factors. It plays a crucial role in carcinogenesis, contributing to the development of tumors in the prostate, lung, pancreas, and breast (27, 28). We show that AA down-regulates GLI1 expression through the modulation of its promoter in an NFATc1-dependent manner. Finally, the blockade of GLI1 results in decreased expression of prosurvival target genes (*BCL2*, *BFL1/A1*, and *4-1BB*), leading to increased cell death both *in vivo* and *in vitro*. Together, these findings define a novel signaling cascade controlling cancer cell survival and help to delineate the mechanisms underlying AA antitumoral properties.

Experimental Procedures

Cell Lines and Culture Conditions—LM3 cells were kindly provided by Dr. Bal de Kier Joffé from the Institute of Oncology Angel H. Roffo (University of Buenos Aires, Buenos Aires, Argentina). PANC1 and MCF7 cell lines were obtained from ATCC and were cultured as reported previously (29–31). L3.6 cells were kindly provided by Dr. Fidler (M. D. Anderson Cancer Center, Houston, TX). For fatty acid treatments, AA, palmitoleic acid (PA), and LA (Nu-Chek Prep, Inc., Elysian, MN) were dissolved in absolute ethanol to an initial dilution of 100 mg/ml. The dilution was prepared under a nitrogen atmosphere and then stored at −80 °C. For all fatty acid treatments, we used 5% fetal bovine serum (FBS) in the cell culture media as a fatty acid carrier. To avoid any issues with the use of FBS, we ran parallel experiments using 0.5 and 1% BSA as a carrier. Both protocols show similar biological effects (data not shown). For some of the experiments, a general caspase (CASP) inhibitor, Q-VD-OPH (SM Biochemicals LLC, Yorba Linda, CA), was used at a final concentration of 20 μM and added at the beginning of the cell culture process. *N*-Acetylcysteine (NAC) and L-glutathione (both from Sigma-Aldrich) were used at final concentration of 500 μM. Cyclosporin A (CsA) and ionomycin (both from Sigma-Aldrich) were used for some of the expression and reporter assays at a concentration of 1 and 0.5 μM, respectively.

Cell Viability Assay—Cell viability was determined by a colorimetric and fluorometric technique using resazurin (Sigma-Aldrich). In each assay, 5×10^4 PANC1 cells/well or 7.5×10^4 MCF7 cells/well were plated in 96-well plates and cultured in their respective media. The following day cells were treated with different concentrations of AA (5, 20, 40, or 60 μg/ml) or the corresponding control vehicle. Twenty-four hours later, resazurin solution was added to each well. Plates were incubated at 37 °C for 4 h, and the fluorescent signal was measured at 560 nm excitation/590 nm emission wavelengths in an FL X800 microplate reader (BioTek Instruments Inc., Winooski, VT). In some viability experiments, cells were treated with 20 μM GANT61 (Selleck Chemicals, Houston, TX) or 20 μM Glabrescione B (kindly provided by Drs. Motta and Di Marcotulio, Sapienza University, Rome, Italy) for 48 h.

In Vivo and in Vitro Apoptosis Assays—In the *in vivo* studies, apoptosis was determined by the terminal deoxyribonucleotidyltransferase-mediated dUTP nick-end labeling (TUNEL) method in which paraffin-embedded tumor tissues were used for the specific detection and quantification of apoptotic cells within a cell population using the DeadEnd™ Fluorometric TUNEL System (Promega, Madison, WI) in accordance with the manufacturer's protocol. Images were obtained using an Axio Observer epifluorescence microscope (Carl Zeiss AG, Oberkochen, Germany). For the *in vitro* studies, apoptosis was determined by DNA fluorescent labeling with Hoechst 33258 (32). Cells (2.5×10^5/well) were plated in 6-well plates and then incubated for 24 h in their respective media. After 24 h of AA treatment or 48 h with GANT61 or Glabrescione B, the medium was removed, and the cells were washed once with PBS and fixed with 500 μl of PBS solution and 500 μl of 3:1 methanol:glacial acetic acid for 5 min. Five hundred microliters of 3:1 methanol:glacial acetic acid was then added for 10 min. The medium was removed, and 1 ml of PBS plus Hoechst 33258 dye was added at a final concentration of 5 μg/ml and then incubated for 10 min at 37 °C before being examined under a fluorescence microscope (Axioskop epifluorescence microscope, Carl Zeiss AG). In addition, the Apo-ONE homogeneous CASP3/7 assay (Promega) was performed. Cells were plated at 5×10^4 cells/well in 96-well plates. After treatment, 100 μl of Apo-ONE CASP3/7 reagent was added to each well containing 100 μl of cells in culture and incubated at room temperature for 6 h. The fluorescent signal was measured at 485 nm excitation/527 nm emission wavelength.

Expression and shRNA Constructs, siRNAs, and Transfection—Expression vectors for NFATc1 and the shRNA constructs were described previously in Elsawa *et al.* (33) and Köenig *et al.* (34). GLI1 expression construct and siRNA targeting GLI1 were described previously (35). The GLI-luciferase reporter containing eight consecutive GLI binding sites upstream of the luciferase gene (GLI-LUC) was kindly provided by Dr. Chi-chung Hui (University of Toronto, Toronto, Ontario, Canada). Human BFL1/A1, 4-1BB, and GLI1 promoter reporter constructs were a gift from Drs. Gelinas (University of Medicine and Dentistry of New Jersey, Piscataway, NJ), Kang (College of Pharmacy, Seoul National University, Seoul, South Korea), and Aberger (University of Salzburg, Salzburg, Austria), respectively. Human *BCL2* promoter containing the −1428 to −799 bp upstream of exon1 was cloned using standard DNA recombinant protocols. Mutations of GLI binding sites in wild type promoters were performed as follows. For *BCL2* promoter, the GLI1 canonical binding sequence from −1125 to −1123 bp was changed from CAC to AAA using the QuikChange II XL site-directed mutagenesis kit (Agilent Technologies, Santa Clara, CA) and the following primers: GGCA-AAGGTGGAGACCTTTAGGAGAAAAAAACCCCAGCG-

TTAGGACGGTGGGCC (sense) and GGCCCACCGTCCTA-ACGCTGGGGTTTTTTTTCTCCTAAAGGTCTCCACCT-TTGCC (antisense). For *BFL1/A1* promoter mutants, two core sequences of the GLI binding sites spanning from −5 to −3 bp and +27 to +29 bp were changed from CAC to AAA using the Q5 site-directed kit (New England Biolabs, Ipswich, MA) and the following set of primers: TTCACATTCCAAACAGCAAT-CTACAAG (sense) and ATGGTACAACCCCTGTGAA-AATG (antisense) and CTAATTTCTCAAAATCCTGCATT-TAAGAC (sense) and AATCCTTGTAGATTGCTGTTTG (antisense), respectively. For the *4-1BB* promoter, the core sequence of the GLI binding site that goes from −12 to −10 bp was changed from CAC to AAA using the primer CCCGCCC-CTGGCTGAGTaaaCGCACTCCTG (sense), the site spanning 510–512 bp was changed from CCC to AAA using the primer TGGTACTGCAAAGTACCTATGAAAGTCAAAAAAAGT-TCTTGCTATTGTTATTTCTGC, and the site from 806 to 808 bp was changed from CAG to AAA using the QuikChange multisite-directed mutagenesis kit (Agilent) and the primer CTTTTGCAGAGTGACATTTGTGAGACAAACTAATTT-GATTAAAATTCTCTTGGAATC (sense). In all cases, mutagenesis was performed according to the manufacturer's protocol, and changes were verified by sequencing.

PANC1 and MCF7 cells were transfected with X-treme-GENE HP (Roche Applied Sciences) according to the manufacturer's instructions. Twenty-four hours prior to transfection, 5×10^4 and 7×10^5 cells were seeded per well in 12-well plates and 100-mm dishes, respectively. For luciferase assays, 2 μg of GLI1, GLI-LUC, BCL2, BFL1/A1, and 4-1BB promoter reporter vectors were used. For transfection of multiple constructs, 10 μg of DNA were used, consisting of 1 μg of promoter reporters and 9 μg of the expression vectors GLI1 and NFATc1. In GLI1 knockdown experiments, 10 μg of shGLI1 or control vector were transfected for 72 h. In the knockdown experiments where GLI1 and NFATc1 siRNAs (FlexiTube siRNA, Qiagen, Valencia, CA) were used along with a non-targeting siRNA negative control (Allstars Negative Control siRNA, Qiagen), cells were transfected using Oligofectamine (Invitrogen) to a final concentration of 100 nM siRNA and harvested 48 h after transfection. In rescue experiments, PANC1 cells were transfected with 10 μg of GLI1 expression construct or empty vector. Twenty-four hours post-transfection, cells were treated with AA at 60 μg/ml for 6 h. Then RNA was extracted to determine the expression of BCL2, BFL1/A1, and 4-1BB.

Luciferase Reporter Assay—Cells were grown and transfected as indicated above. For the assays, cells were plated in triplicate at 5×10^4 cells/well in 12-well plates in the corresponding medium. After 24 h of transfection, cells were treated with AA, and then samples were harvested and prepared for luciferase assays in accordance with the manufacturer's protocol (Promega). The total protein of samples in each well was quantitated using the Bio-Rad protein assay, and luciferase readouts were normalized to protein content. Relative luciferase activity represents luciferase/protein concentration readouts normalized to control group within each experiment (36).

Quantitative Reverse Transcription-PCR (q-PCR)—Total RNA was extracted from LM3 tumors and cultured cells using TRIzol reagent (Invitrogen). The High-Capacity cDNA Reverse Transcription kit (Applied Biosystems, Carlsbad, CA) was used to reverse transcribe 5 μg of RNA. A portion of the total cDNA was amplified by real time PCR. Samples were prepared with PerfeCTa SYBR Green FastMix (Quanta BioSciences Inc., Gaithersburg, MD) and the following primer sets: m18S: sense, AACCCGTTGAACCCCATTCGTGAT; antisense, CAGGT-TCACCTACGGAAACCTTGT; mGli1: sense, CCTGGACA-ACACTCAGCTGGACTT; antisense, GGAAATACCATCT-GCTTGGGGTTC; m4-1bb: sense, AGTGTCCTGTGCATG-TGA; antisense, AGTTATCACAGGAGTTCTGC; mBcl2: sense, TGAGTACCTGAACCGGCATCT; antisense, GCATC-CCAGCCTCCGTTAT; mBfl1/a1: sense, TGCCAGGGAAG-ATGGCTGAG; antisense, TCCGTAGTGTTACTTGAG-GAG; hGAPDH: sense, GACCTGACCTGCCGTCTAGAA-AAA; antisense, ACCACCCTGTTGCTGTAGCCAAAT; hGLI1: sense, TGCCTTGTACCCTCCTCCCGAA; antisense, GCGATCTGTGATGGATGAGATTCCC; hBCL2: sense, GAGCCACGACCCTTCTTAAGACAT; antisense, CAGGG-GTCAATTAATCCATGACA; h4-1BB: sense, ATGACAATA-AGCCACGAGGTGCAG; antisense, AAAGGGAGCAGGAC-AAAGGCAGAA; hBFL1/A1: sense, TTTGCTCTCCACCAG-GCAGAAGAT; antisense, GGCAGTGTCTACGGACACAA-CATT; hNFATc1: sense, CCGAGCCCACTACGAGA; anti-sense, CCGCCGTCCCAATGAAA.

Amplification was performed using the C1000 Thermal Cycler (Bio-Rad). Each RNA level was normalized by comparison with the corresponding housekeeping RNA level in the same sample. The results were calculated following the 2ΔCt method.

Chromatin Immunoprecipitation (ChIP) Assay—ChIP was conducted following a modified version of the Magna ChIP kit protocol (EMD Millipore, Bedford, MA). Briefly, PANC1 cells (7×10^6) were cross-linked with 1% formaldehyde directly into the medium for 10 min at room temperature. The cells were then washed and scraped with PBS, collected by centrifugation at 800 × *g* for 5 min at 4 °C, resuspended in cell lysis buffer, and incubated on ice for 15 min. The pellet was then resuspended in nuclear lysis buffer and sheared to fragment DNA to ~700 bp. Samples were then immunoprecipitated using a GLI1 antibody (Novus Biologicals, Littleton, CO), NFATc1 antibody (Santa Cruz Biotechnology, Santa Cruz, CA), normal rabbit IgG (EMD Millipore), or normal mouse IgG (EMD Millipore) overnight at 4 °C on a rotating wheel. Following immunoprecipitation, cross-links were removed, and immunoprecipitated DNA was purified using spin columns and subsequently amplified by PCR. PCR was performed using a primer set to amplify a 350-bp region of the *GLI1* promoter containing a potential NFATc1 binding site (sense, AGCAGTATAGGGTCCCTCAAG; antisense, CGCGAGAAGCGCAAACT) and primer sets to amplify *BCL2*, *BFL1/A1*, and *4-1BB* promoters containing potential GLI1 binding sites as follows: *BCL2*: sense, ACACACGTCTG-CGAGTGTGAATGT; antisense, TCCCTCTGTCCCTAAC-ACCTTT; *BFL1/A1*: sense, GAGTATCTGTTGGGTGTATA-CCTATG; antisense, GATGATACATGGAGGCTGGTG-GAA; *4-1BB*: sense, ATCTGTGACACATCCTGACAGTAGA; antisense, ACATGTGGAAAGACCTCCCTGTTC; sense; GAACAGGGAGGTCTTTCCACATGT; antisense, TGATG-

AAATCTGGCACAGGTATGAT. PCR products were visualized using a 2% agarose gel.

For the transient ChIP assay, PANC1 cells (1×10^6) were grown overnight in 100-mm dishes and then transfected with 3 μg of the BCL2, 4-1BB, or BFL1/A1 promoter reporter vectors with WT or mutant GLI1 biding sites using X-tremeGENE HP. Twenty-four hours after transfection, cells were cross-linked with formaldehyde and harvested, and chromatin immunoprecipitations were performed as described above. Antibodies used in the procedure include anti-GLI1 (Novus) and anti-rabbit IgG (EMD Millipore). The resulting DNA was analyzed by real time PCRs with the same set of primers described previously. Quantitative SYBR PCR was performed in triplicate for each sample using the C1000 Thermal Cycler. Results are represented as -fold of enrichment where each antibody signal was relative to its respective input and then normalized to the non-immune IgG control signal.

Immunoblotting—Western blotting was performed as described previously (28, 36). 1×10^6 PANC1 and MCF7 cells were plated in standard medium with 10% FBS and used 24 h later for treatment or transfection experiments. Cells were lysed 48 h after transfection. GLI1 and NFATc1 antibodies were obtained from Cell Signaling Technology (Danvers, MA). BCL2 antibody was purchased from Bethyl Laboratories (Montgomery, TX), and BFL1/A1 and 41BB antibodies were obtained from Abcam (Cambridge, MA). Anti-α-tubulin was obtained from Sigma-Aldrich. Peroxidase-conjugated secondary antibodies were used, and immunoreactive proteins were detected by chemiluminescence (GE Healthcare).

Fluorescence Microscopy—PANC1 cells were transfected for 48 h with an NFATc1-GFP expression construct (Addgene, Cambridge, MA). Cells were treated with NAC, ionomycin, CsA, or AA as described above and in figure legends. PANC1 cells were then fixed in 4% formaldehyde and mounted in Prolong with DAPI (Invitrogen). Microscopy was performed using an Olympus AX70 equipped with a Hamamatsu C4742-95 camera. Images were captured using MetaMorph (version 7.3.2; Universal Imaging Corp.) and analyzed with ImageJ.

In Vivo Studies—BALB/c mice were housed in groups of two to four in polycarbonate cages. Food and water were provided *ad libitum*. Animals were maintained at a constant temperature of 20 °C and subjected to a 12-h light-12-h darkness cycle. Animal studies were conducted in accordance with the guidelines of the National Institutes of Health Guide for the Care and Use of Laboratory Animals, and all the procedures were approved by the Institutional Committee for the Care and Use of Laboratory Animals of the School of Medicine, University of Cordoba, Argentina.

Three-month-old mice were inoculated subcutaneously in the left flank with 1×10^6 viable LM3 murine mammary adenocarcinoma cells with lung moderate metastatic capability (31) in 0.02 ml serum-free minimum Eagle's medium. When tumors became palpable, mice were randomized in treatment or control groups. The treatment group ($n = 10$) received pure AA at a dose of 0.70 mg AA/g of body weight injected in the tumor bed every 7 days over 21 days. The control group ($n = 7$) received injections of normal saline buffer in the tumor bed. The experimental period of 21 days was determined according to the time required for the generation of metastasis and before the tumor reaches the maximum standard size allowed. Tumor volume was measured with digital slide calipers at the beginning of treatment and every 7 days for 3 weeks. The tumor volume was calculated from the transverse (width) and longitudinal (length) diameters in millimeters of the tumor using the formula: Volume = Length $\times$ Width^2/2 (37). Twenty-one days after treatment, the animals were sacrificed. The tumors and lungs were rapidly removed, and samples preserved in formalin for subsequent H&E histopathological analysis and immunohistochemical studies.

We also evaluated the potential acute toxicity after AA administration through examination of general conditions, body weight, food intake, and mortality. Major organs were examined macroscopically, and lung, liver, and spleen were fixed and stained with H&E for histopathological examination (38). We determined that the dose used in this study was well tolerated by the experimental mice and had no toxicity. All mice survived until the end of the experimental study, and no adverse effects were observed. Mice displayed normal behavior, normal feeding, normal energy, and shining hair. Also, AA-treated animals as well as controls showed no weight loss, no salivation or vomiting, no mouth or nose dryness or edema, no eye secretion or running nose, and no flare or ulceration in the skin. At necropsy, no alteration or significant difference was recorded in internal organ evaluation. Moreover, histopathological analysis of the different tissue showed no significant changes compared with the control group.

For the GANT61 experiment, tumors were inoculated following the above protocol. When tumors were palpable, mice were randomized and treated daily with GANT61 at a dose of 50 mg/kg of body weight. The control group received injections of normal saline buffer in the tumor bed. The experimental period of 21 days was determined according to the time required for the generation of metastasis and before the tumor reaches the maximum standard size allowed. Tumor volume was measured with digital slide calipers at the beginning of treatment and every 7 days for 3 weeks.

Ferric Xylenol Orange Peroxide Assay—To determine the levels of hydroperoxides, we measured the dye xylenol orange and Fe^{3+} generated as an iron-xylenol orange complex in the visible absorbance range. For the assay, 5×10^4 cells/well were plated in a 96-well plate, and 24 h later cells were treated with AA for 24 h as we detailed above. Cells were lysed with 10 μl of 1% (v/v) SDS and mixed with the appropriate volume of reagents to give final concentrations of 25 mM H_2SO_4, 100 mM xylenol orange, and 250 mM ferrous ammonium sulfate. After 30 min in the dark, the absorbance was read at 560 nm with xylenol orange as a blank with a GloMax multimode microplate reader (Promega) (39).

γ-Glutamyl Transpeptidase Activity—γ-Glutamyl transpeptidase activity was measured based on the principle that γ-glutamyl-*p*-nitroanilide acts as a donor and glycylglycine acts as an acceptor substrate (40). Five thousands cells/well were plated in a 96-well plate. After attachment, the cells were treated with AA for 24 h as detailed above. A kinetic modified Szasz method was performed according to the kit instructions of γ-G-test cinética AA (Wiener Laboratorios, Rosario, Santa Fe, Argen-

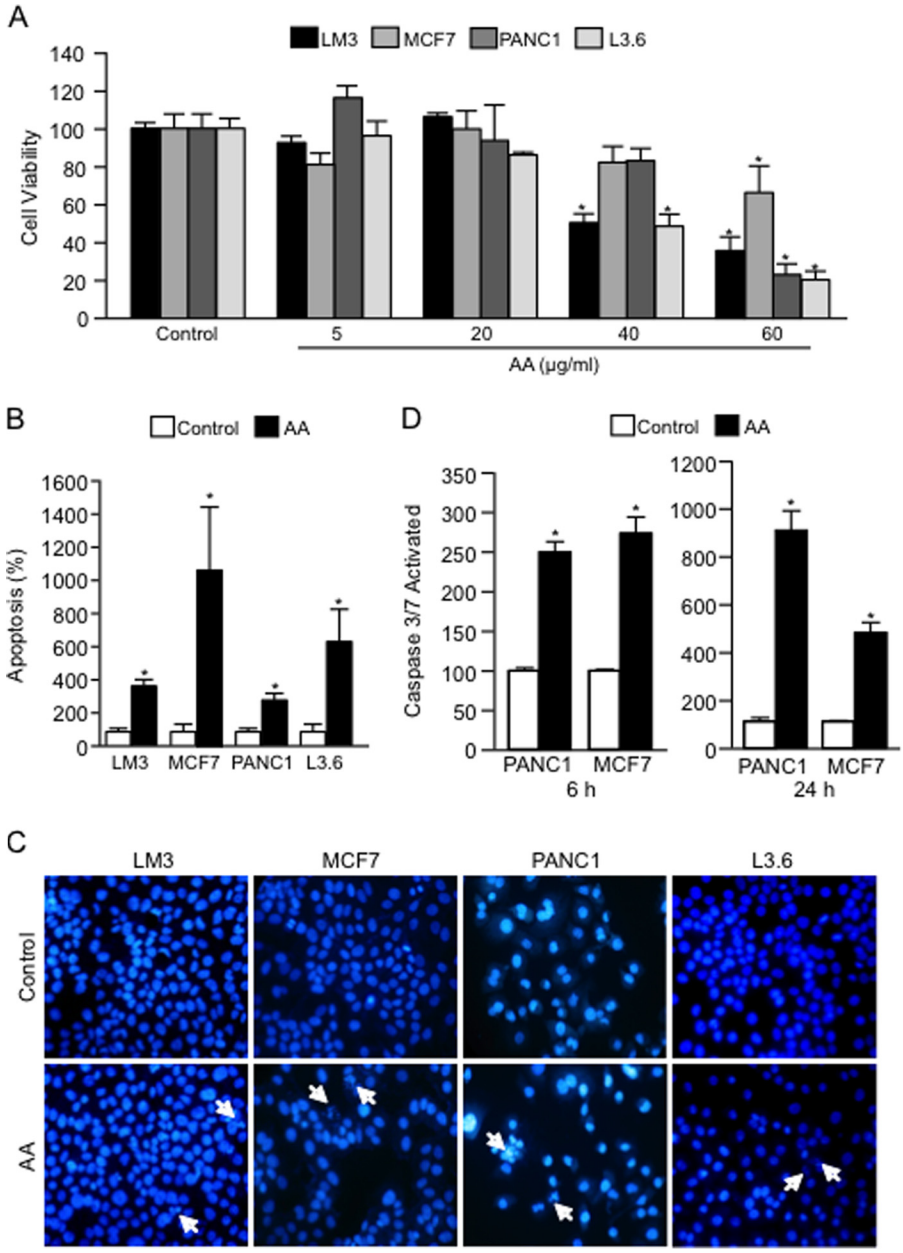

FIGURE 1. **AA treatment induces apoptosis *in vitro*.** *A*, LM3, MCF7, PANC1, and L3.6 cells were treated with the control vehicle (ethanol) or different concentrations of AA (5, 20, 40, and 60 μg/ml). Cells were treated for 24 h, and viability was determined by the fluorometric indicator dye resazurin to measure the metabolic capacity of cells. These cells show a significant reduction in viability after a treatment concentration of 60 μg/ml AA for MCF7 and PANC1 and 40 μg/ml AA for LM3 and L3.6 compared with controls. *Bars* and *error bars* represent means and S.E., respectively; $n = 3$. *, $p < 0.05$ *versus* control group. *B* and *C*, apoptosis was evaluated by fluorescence staining with Hoechst 33258 in cells treated for 24 h ±AA. *B*, cells were cultured in 6-well plates (2.5×10^5 cells/well) and treated with 60 μg/ml AA for MCF7 and PANC1 and 40 μg/ml AA for LM3 and L3.6 cells. Apoptosis was measured by counting the number of apoptotic nuclei/total nuclei and normalizing the data by control values (control = 100%). *Bars* and *error bars* represent means and S.E., respectively; $n = 3$. *, $p < 0.05$ *versus* control group (EtOH). *C*, representative images showing increased apoptotic nuclei in AA-treated cells. *Arrows* indicate apoptotic nuclei. *D*, apoptosis was evaluated in MCF7 and PANC1 cells treated for 6 (*left panel*) and 24 h (*right panel*) by Apo-ONE homogeneous CASP3/7 assay. Cells were plated at 5×10^4 cells/well in 96-well plates. Fluorescent signals were measured at a wavelength of 485 nm excitation/527 nm emission). *Bars* and *error bars* represent means and S.E., respectively; values are normalized by control values (control = 100%); $n = 5$. *, $p < 0.05$ *versus* control group (EtOH).

tina). The kinetics of the reaction was determined measuring the absorbance at 450 nm at time 0 and after 10 and 20 min with a GloMax multimode microplate reader. Total protein was determined by Bradford assay. The γ-glutamyl transpeptidase specific activity was presented in γ-glutamyl transpeptidase international units (IU) = ΔA/min × 1.158 IU of GGPT/mg of proteins (41).

Statistical Analysis—Analysis of variance models were used to evaluate differences among the experimental groups followed by the Duncan test for mean comparisons ($p < 0.05$). All experiments were performed in triplicate and repeated at least twice unless otherwise noted. For the *in vivo* experiments, a generalized estimating equation model was used with γ distribution for random component and link function identity. Time, treatment, and their interaction were the co-varieties in the lineal predictor. The statistical analyses were performed using InfoStat 2012 software (Grupo InfoStat, Universidad Nacional de Cordoba, Cordoba, Argentina).

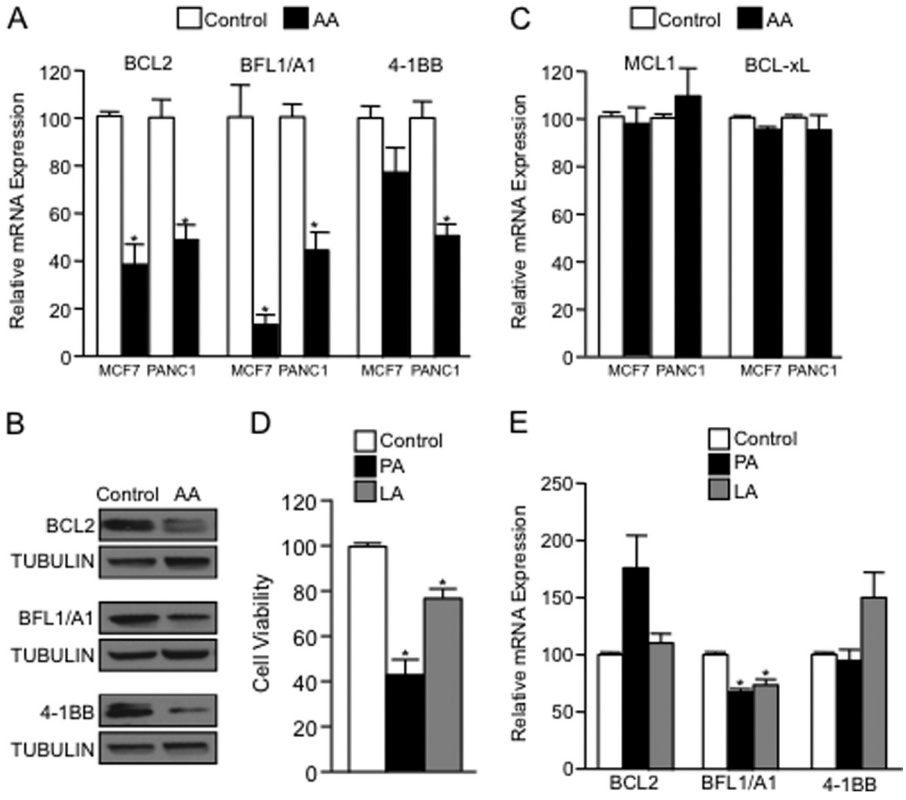

FIGURE 2. **AA decreases antiapoptotic BCL2, BFL1/A1, and 4-1BB expression.** *A*, BCL2, BFL1/A1, and 4-1BB mRNA expression levels were determined by RT-q-PCR. PANC1 and MCF7 cells were treated ±AA (60 μg/ml) or the control vehicle for 6 h. *Bars* and *error bars* represent means and S.E., respectively; $n = 3$. *, $p < 0.05$ *versus* control group (EtOH). *B*, immunoblotting analysis showed lower levels of BCL2, BFL1/A1, and 4-1BB protein expression in MCF7 cells treated with AA compared with the vehicle control at 6 h post-treatment. *C*, expression of MCL1 and BCL-xL were determined by q-PCR in PANC1 and MCF7 cells treated with vehicle or AA (60 μg/ml). *D*, PANC1 cells were treated with the control vehicle (ethanol), PA, or LA (both at 60 μg/ml). Cells were treated for 24 h, and viability was determined by the fluorometric indicator dye resazurin. These cells show a significant reduction in viability after PA and LA treatments. *Bars* and *error bars* represent means and S.E., respectively; $n = 3$. *, $p < 0.05$ *versus* control group. *E*, expression of the indicated genes in PANC1 cells treated with PA and LA was determined as described in *A*.

Results

AA Treatment Induces Apoptosis in Vitro—Using *in vitro* models, we demonstrated that AA decreased cell viability in both LM3 and MCF7 mammary cancer cell lines and in pancreatic cancer cell lines PANC1 and L3.6. Cancer cell viability was reduced in a dose-dependent manner in all cell lines tested (Fig. 1*A*). Further analysis shows that AA induced apoptosis after 24 h of treatment as measured by nuclear fragmentation (Fig. 1, *B* and *C*) with a significant increase ($p < 0.05$) at a concentration of 60 μg/ml in PANC1 and MFC7 cell lines and 40 μg/ml in LM3 and L3.6 cell lines relative to controls, concentrations found to have significant effects in the previous cell viability experiments. In addition, in PANC1 and MCF7 cell lines, AA treatment elicited a significant increase in CASP3/7 activity after 6 (*left panel*) and 24 h (*right panel*) of treatment (Fig. 1*D*). Taken together, these data support a role for AA as an anticancer agent by affecting cell growth and inducing apoptosis.

AA Treatment Decreases the Expression of Antiapoptotic Molecules BCL2, BFL1/A1, and 4-1BB—To define the mechanisms behind AA-induced apoptosis, we examined by q-PCR the expression of a set of genes with a known role in regulation of cell growth and apoptosis. We identified the antiapoptotic molecules BCL2, BFL1/A1, and 4-1BB (42, 43) as down-regulated in AA-treated cells. As shown in Fig. 2*A*, AA treatment of MCF7 and PANC1 cells decreased BCL2, BFL1/A1, and 4-1BB mRNA levels compared with controls. A significant difference ($p < 0.05$) was observed in all genes with the exception of the 4-1BB antiapoptotic gene in MCF7 cells, the levels of which showed a tendency to decrease. Immunoblot analysis shows a similar effect of AA on the protein expression of these antiapoptotic molecules (Fig. 2*B*). This effect was specific for these molecules as the expression of other antiapoptotic proteins, MCL1 and BCL-xL, was not affected by the AA treatment (Fig. 2*C*). Next we determined whether these effects of AA were also shared by other fatty acids with known antitumoral activity, PA and LA. Similar to AA, these fatty acids decrease viability in PANC1 cells (Fig. 2*D*) but do not significantly change the expression of the antiapoptotic molecules except BFL1/A1, which is down-regulated by the treatment with PA and LA (Fig. 2*E*).

BCL2, BFL1/A1, and 4-1BB Are Direct Targets of GLI1—Bioinformatics analysis of the promoters of *BCL2*, *BFL1/A1*, and *4-1BB* identified the transcription factor GLI1 as a candidate regulator of the expression of these molecules (Fig. 3*A*). To define the role of GLI1 in antiapoptotic *BCL2*, *BFL1/A1*, and *4-1BB* promoter genes, we utilize a combination of reporter, expression, and chromatin assays. Using two independent shRNA constructs targeting GLI1, we showed that knockdown of GLI1 diminished BCL2, BFL1/A1, and 4-1BB mRNA expression in PANC1 cells (Fig. 3*B*). Similar results were obtained

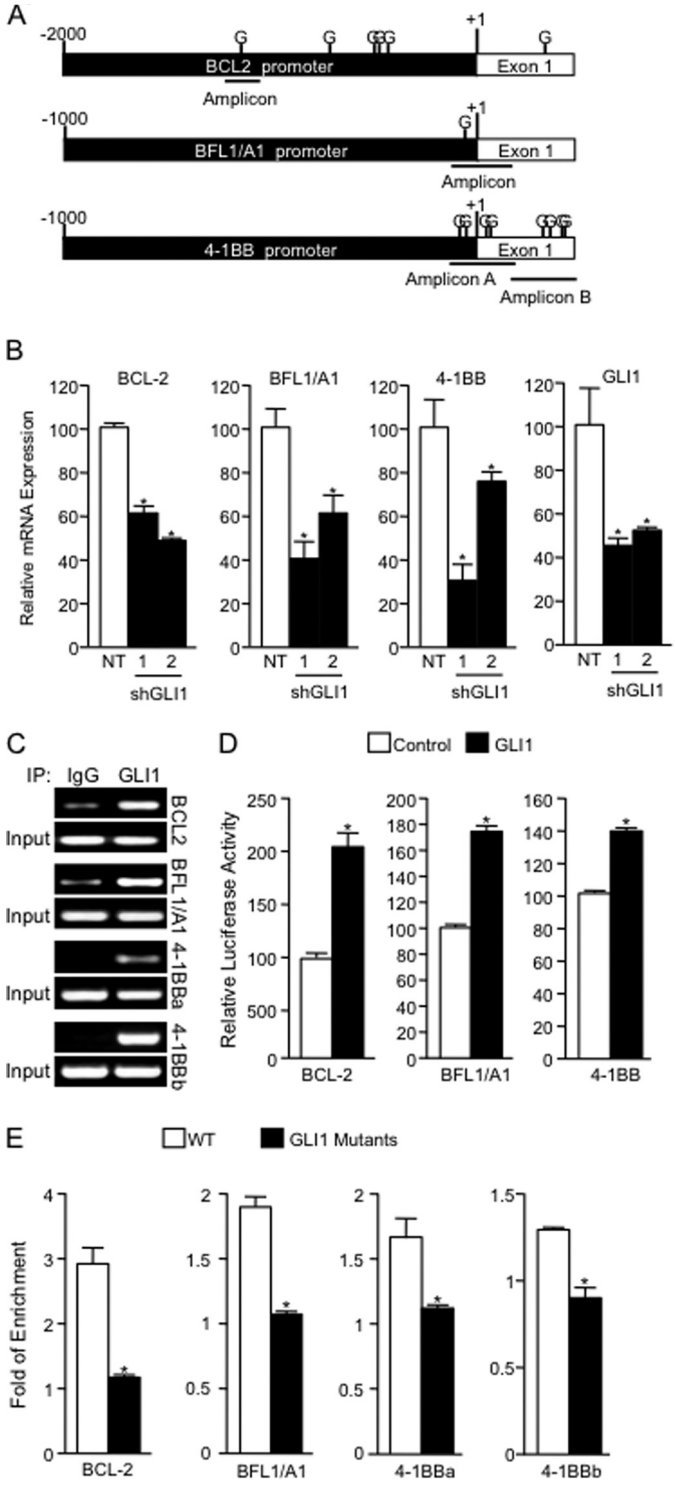

FIGURE 3. **BCL2, BFL1/A1, and 4-1BB are direct targets of the transcription factor GLI1.** *A*, bioinformatics analysis of the *BCL2*, *BFL1/A1*, and *4-1BB* promoters identified candidate GLI (*G*) binding sites upstream of their first exon. *B*, PANC1 cells transfected with two different shRNA vectors targeting GLI1 (shGLI1 and shGLI2) and a non-targeting control vector (*NT*) were examined for BCL2, BFL1/A1, and 4-1BB mRNA expression levels by q-PCR. *Bars* and *error bars* represent means and S.E., respectively; $n = 3$. *, $p < 0.05$ *versus* non-targeting control. *C*, PANC1 cells were lysed, and a ChIP assay was performed using a GLI1 antibody (*GLI1*) or IgG control (*IgG*). PCR was performed using specific sets of primers for *BCL2*, *BFL1/A1*, and *4-1BB* promoter regions as indicated under "Experimental Procedures." *IP*, immunoprecipitation. *D*, relative changes in luciferase activity in PANC1 cancer cells co-transfected with promoter reporter constructs of the antiapoptotic genes (BCL2, BFL1/A1, and 4-1BB) and with the GLI1 expression constructs or control vector. Data are mean ± S.E.; $n = 3$. *, $p < 0.05$ *versus* the control group. *E*, transient ChIP assay in PANC1 cells transfected with the WT BCL2, BFL1/A1, and 4-1BB promoter reporter constructs or mutants lacking GLI1 binding sites. *Bars* and *error bars* represent means and S.E., respectively; $n = 3$. *, $p < 0.05$ *versus* the control group.

using an siRNA targeting GLI1 (data not shown). A ChIP assay confirmed the binding of endogenous GLI1 to a region located −1234 to −1025 bp upstream of the first exon for *BCL2*, −121 to +226 bp from the first exon for *BFL1/A1*, and two regions for *4-1BB* located −192 to +341 bp (a) and +317 to +873 bp (b) from the first exon (Fig. 3*C*). In addition, overexpression of GLI1 led to an increase in the promoter activity of BCL2, BFL1/A1, and 4-1BB in reporter assays (Fig. 3*D*). Finally, to demonstrate the specificity of the GLI1 binding sites identified for each gene promoter, we utilized a transient ChIP (44) using WT promoter construct and mutant versions of these vectors lacking the GLI1 binding sites. In each case, we found a decreased binding of GLI1 to the mutant promoters compared with their WT sequence (Fig. 3*E*). These results confirm a previously known GLI1 target gene (*BCL2*) (45) and demonstrate that *BFL1/A1* and *4-1BB* are novel direct targets of GLI1 transcription factor.

AA Diminishes GLI1 Expression by Inducing the Repressor Activity of NFATc1—To determine whether GLI1 plays a role in the AA-induced down-regulation of antiapoptotic genes, we investigated the effect of AA treatment on GLI1 expression and activity. We observed that AA treatment decreased the mRNA expression of GLI1 in PANC1 and MCF7 cells (Fig. 4*A*). This effect was specific to AA as LA and PA did not repress GLI1 mRNA expression (data not shown). GLI1 protein expression was also reduced by AA as shown by Western blot analysis in PANC1 cells at 6 and 24 h post-treatment with AA (Fig. 4*B*). Altered GLI1 expression was accompanied by a decrease in GLI1-associated transcriptional activity as demonstrated by lower activity of the GLI luciferase reporter (GLI-LUC) in AA-treated cells (Fig. 4*C*). To rule out the possibility that the effect of AA on GLI1 activity was a consequence of cells undergoing apoptosis, we performed the AA treatment in the presence of a CASP inhibitor (Q-VD-OPH). AA was able to decrease GLI1 activity even in the presence of Q-VD-OPH as shown in Fig. 4*C*. As a control for these treatments, we measured the levels of activated CASP3/7 and cell viability, which were altered by AA treatment but restored to basal levels by the CASP inhibitor (Fig. 4*D*). Next, we sought to determine whether GLI1 overexpression was able to block AA induction of cell death. As shown in Fig. 4*E*, GLI1 overexpression in PANC1 cells was able to reverse AA-induced CASP3/7 activation. Similarly, overexpression of GLI1 restored the expression of BCL2, BFL1/A1, and 4-1BB in cells treated with AA (Fig. 4*F*). Finally, we demonstrated that pharmacological or genetic inhibition of GLI1 mimics the effect of AA on cell growth. Knockdown of GLI1 led to an increase in the number of apoptotic cells in both PANC1 and MCF7 lines (Fig. 4*G*). Treatment of these cells with GLI1 inhibitors GANT61 (Fig. 4*H*) and Glabrescione B (Fig. 4*I*) led to decreased cell viability. Collectively, these results suggest that down-regulation of GLI1 is required for AA induction of cell death.

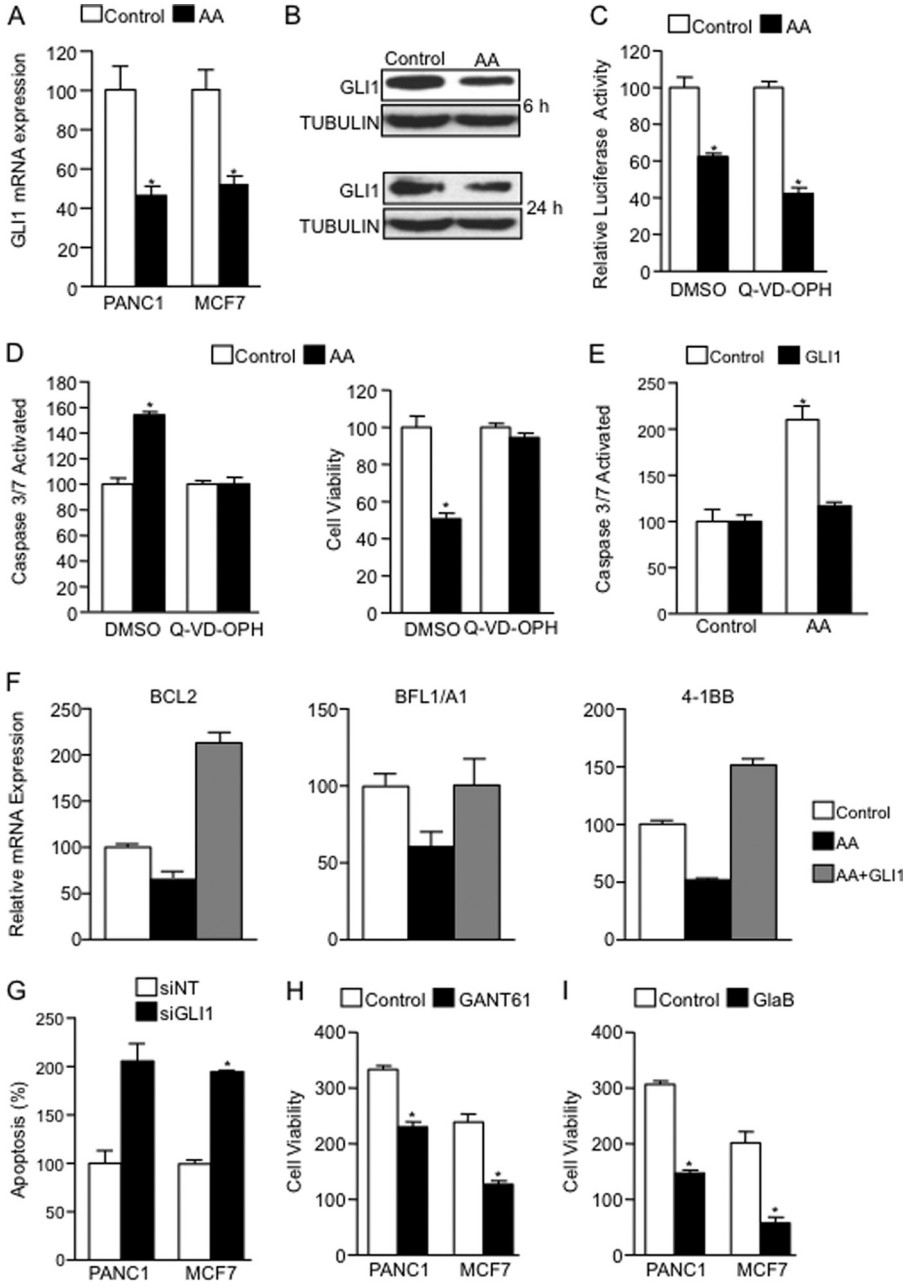

FIGURE 4. **AA decreases GLI1 expression.** *A*, GLI1 mRNA expression levels were determined by real time RT-PCR in PANC1 and MCF7 cells treated with AA (60 μg/ml) or the control vehicle for 3 h. *Bars* and *error bars* represent means and S.E., respectively; $n = 3$. *, $p < 0.05$ *versus* control group (EtOH). *B*, Western blot analysis shows that AA decreases GLI1 protein expression at 6 and 24 h post-treatment. *C*, relative changes in luciferase activity in PANC1 cancer cells transfected with a GLI-LUC reporter and subsequently treated with the CASP inhibitor Q-VD-OPH at 20 μM or the control vehicle DMSO and co-treated with AA (60 μg/ml) or control vehicle (EtOH) for 6 h. *Bars* and *error bars* represent means and S.E., respectively; $n = 3$. *, $p < 0.05$ *versus* control group. *D*, apoptosis was measured by homogeneous CASP3/7 assay and viability was measured by resazurin assay in PANC1 cells treated with the CASP inhibitor Q-VD-OPH at 20 μM. Cells were subsequently co-treated with AA (60 μg/ml) or control vehicle for 6 h. *Bars* and *error bars* represent means and S.E., respectively; $n = 3$. *, $p < 0.05$ *versus* control group. *E*, PANC1 cells were transfected with the GLI1 expression construct or the control vector. After 24 h, transfected cells were treated with AA at 60 μg/ml or control vehicle (EtOH) for 6 h. A homogeneous CASP3/7 assay was performed to measure apoptosis. *Bars* and *error bars* represent means and S.E., respectively; $n = 3$. *, $p < 0.05$ *versus* control vector. *F*, mRNA expression of BCL2, BFL1/A1, and 4-1BB in PANC1 and MCF7 cells transfected with GLI1 expression construct and control vector and treated with AA at a concentration of 60 μg/ml. *G*, apoptosis was evaluated by fluorescence staining with Hoechst 33258 in PANC1 and MCF7 transfected with siRNA non-targeting (*siNT*) control and siGLI1. Cell viability was measured by resazurin assay (*right panel*) in PANC1 cells treated with GANT61 at 20 μM (*H*) or Glabrescione B (*GlaB*) (*I*) at 20 μM for 48 h. *Bars* and *error bars* represent means and S.E., respectively; $n = 3$. *, $p < 0.05$ *versus* control group.

The above results demonstrated that AA modulates the expression and activity of GLI1 in cancer cells. Further analysis showed that AA decreased the transcriptional activity of the *GLI1* promoter in PANC1 (*left*) and MCF7 (*center*) starting after 30 min and maintained up to 6 h (Fig. 5*A*). Even upon CASP inhibition, AA treatment decreased GLI1 promoter activity (Fig. 5*B*). Reporter studies using deletion constructs of this promoter defined an area located −200/−100 bp upstream of exon 1 as the AA-responsive element (Fig. 5*C*). *In silico* examination of transcription factor binding sites in this region

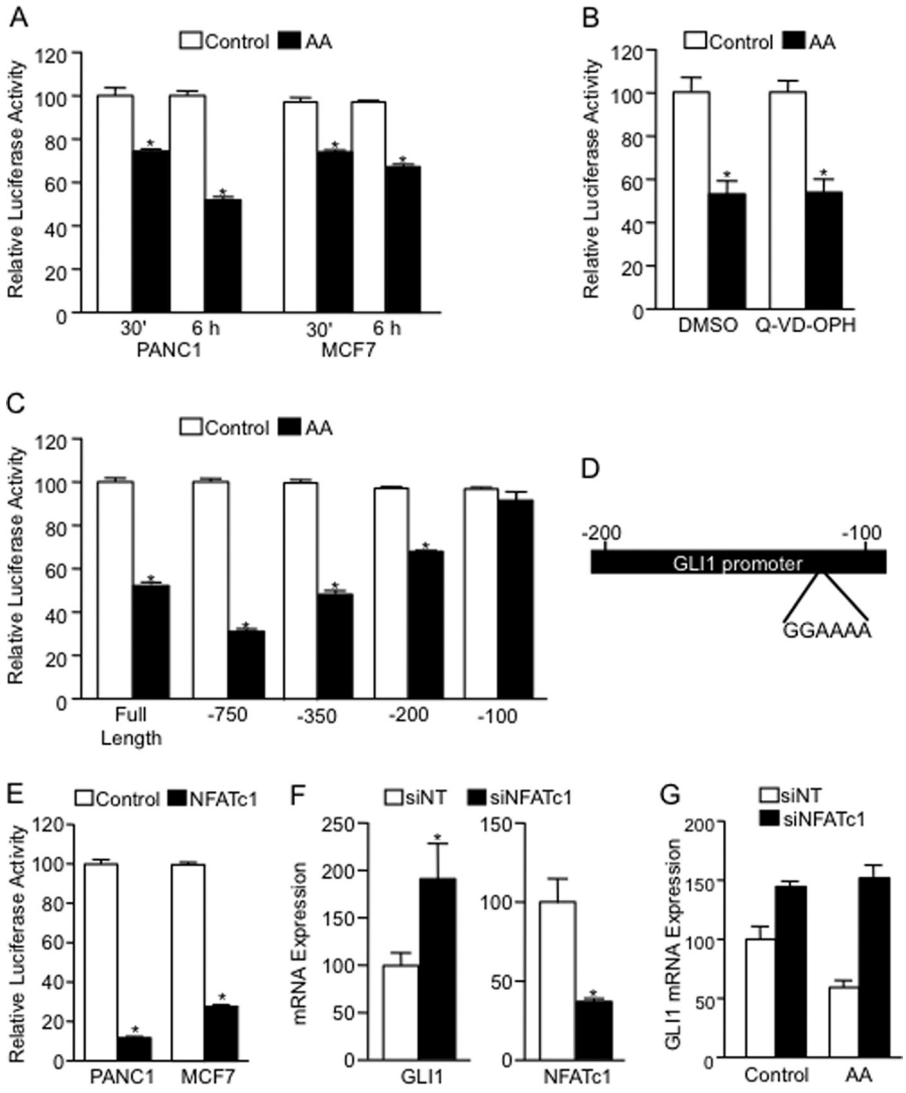

FIGURE 5. **AA represses GLI1 promoter activity in cancer cells.** *A*, relative changes in luciferase activity in PANC1 (*left*) and MCF7 (*right*) cancer cells transfected with GLI1 promoter reporter vector and subsequently treated with AA (60 μg/ml) or control vehicle (EtOH) for 30 min (′) and 6 h. *Bars* and *error bars* represent means and S.E., respectively; $n = 3$. *, $p < 0.05$ *versus* the control group. *B*, relative changes in luciferase activity in PANC1 cancer cells transfected with a GLI1 promoter reporter and subsequently treated with the CASP inhibitor Q-VD-OPH at 20 μM or the control vehicle DMSO and co-treated with AA (60 μg/ml) or the control vehicle (EtOH) for 6 h. *Bars* and *error bars* represent means and S.E., respectively; $n = 3$. *, $p < 0.05$ *versus* the control group. *C*, relative luciferase activity in PANC1 cells transfected with a series of truncated GLI1 promoter reporter constructs and then treated with AA or control (EtOH). *, $p < 0.05$ *versus* the control group. *D*, diagram showing AA-responsive region and NFATc1 binding site within the *GLI1* promoter. *E*, relative changes in luciferase activity in PANC1 and MCF7 cancer cells co-transfected with the GLI1 promoter reporter and with the NFATc1 expression constructs or PCMV control vector. *Bars* and *error bars* represent means and S.E., respectively; $n = 3$. *, $p < 0.05$ *versus* the control group. *F*, PANC1 cells transfected with an siRNA targeting NFATc1 or a non-targeting control (*siNT*) were examined for GLI1 and NFATc1 mRNA expression levels by real time RT-PCR. *Bars* and *error bars* represent means and S.E., respectively; $n = 3$. *, $p < 0.05$ *versus* non-targeting control. *G*, GLI1 mRNA and NFATc1 expression levels were determined by q-PCR in PANC1 transfected with a non-targeting (*siNT*) control and siRNA targeting NFATc1 and then treated with AA (60 μg/ml) or the control vehicle for 3 h. *Bars* and *error bars* represent means and S.E., respectively; $n = 3$ expressed as relative percentage to control. *, $p < 0.05$ *versus* control group (EtOH).

(TESS and Tfsitescan database programs) identified NFATc1 as a candidate mediator of AA regulation of the *GLI1* promoter in cancer cells (Fig. 5*D*). Overexpression of NFATc1 indeed caused a dramatic decrease in GLI1 promoter activity in both PANC1 and MCF7 cells (Fig. 5*E*). Conversely, siRNA knockdown of NFATc1 increased the expression of GLI1 (Fig. 5*F*). We also found that AA requires NFATc1 to decrease GLI1 expression by showing that knockdown of NFATc1 impairs AA-induced reduction of GLI1 (Fig. 5*G*). Next, we showed that NFATc1 nuclear translocation was increased upon administration of AA (Fig. 6*A*), and NFATc1 binding to a region located −200/−100 bp upstream of the first exon of *GLI1* was increased by treatment with this fatty acid (Fig. 6*B*). These studies indicate that AA suppresses GLI1 expression via NFATc1 binding to the *GLI1* promoter.

NFATc1 activation is often mediated by the phosphatase calcineurin (46, 47). Thus, we next investigated the involvement of calcineurin in the AA-initiated repression of GLI1 expression. We found that treatment with the calcineurin inhibitor CsA inhibited the nuclear localization of NFATc1 and rescued the AA-mediated down-regulation of GLI1 expression in PANC1 cells (Fig. 6*C*, *right panel*). Conversely, treatment with the calcium ionophore ionomycin, which is known to activate calcineurin (46, 48), stimulated NFATc1 nuclear translocation

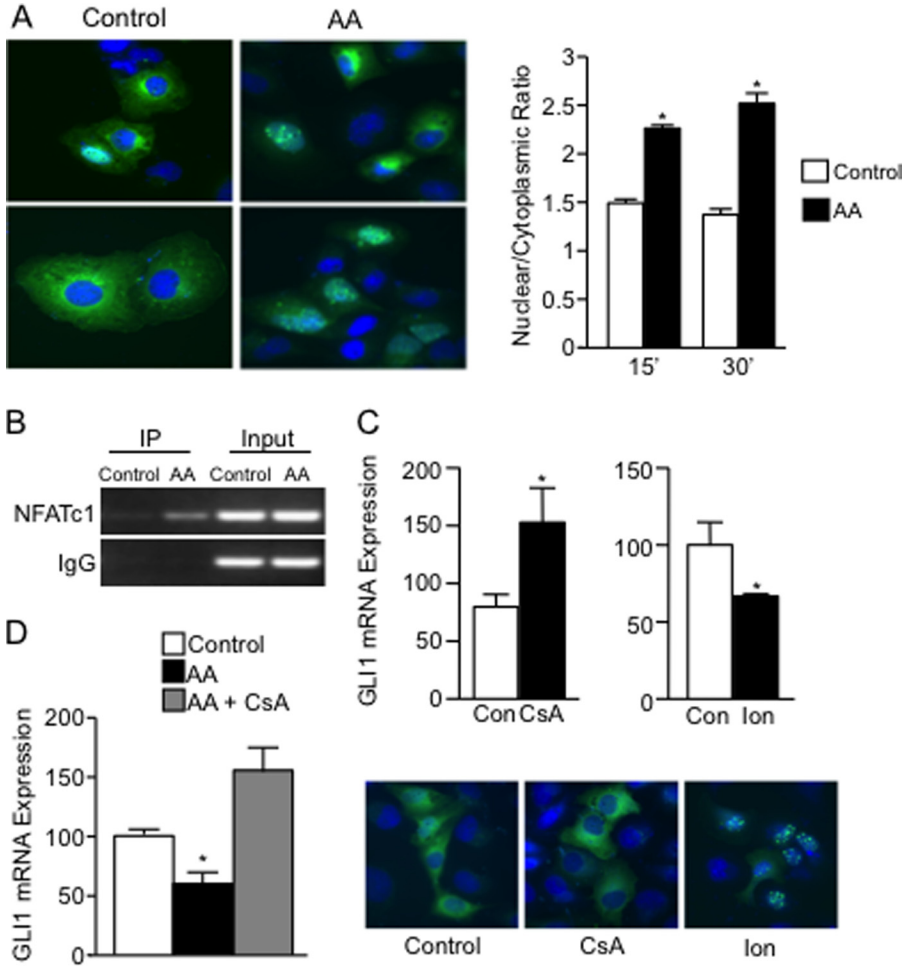

FIGURE 6. **NFATc1 mediates AA silencing of GLI1 expression.** *A*, PANC1 cells were transfected with an expression construct encoding NFATc1-GFP for 48 h and then treated with AA (60 μg/ml) or vehicle for 15 or 30 min. Cells were fixed, stained with DAPI, and then viewed by fluorescence microscopy. *Left panel*, two examples each of NFATc1-GFP fluorescence in 15-min control and AA-treated cells are shown. *Green*, NFATc1-GFP; *blue*, DAPI. *Right panel*, nuclear/cytoplasmic localization of NFATc1 was quantified by image analysis of micrographs as in *A*. $n \geq 40$ cells for each condition. *, $p < 0.05$ *versus* the control group. *B*, ChIP assay was performed in PANC1 lyses cells pretreated with AA (60 μg/ml) or control vehicle (EtOH) for 6 h; NFATc1 antibody or IgG control antibody was used. PCR was performed using a specific set of primers indicated under "Experimental Procedures" for the −350 bp upstream *GLI1* promoter region. *IP*, immunoprecipitation. *C*, PANC1 cells were treated for 3 h with 1 μM CsA or 0.5 μM ionomycin (*Ion*) for 15 min (′) or vehicle control (*Con*) and examined for GLI1 mRNA expression by q-PCR (*upper panel*). PANC1 cells transfected with NFATc1-GFP for 48 h were similarly treated with CsA, ionomycin, or vehicle and viewed by fluorescence microscopy (*lower panel*) to validate the effects of these treatments on NFATc1 localization. *Green*, NFATc1-GFP; *blue*, DAPI. *D*, PANC1 cells were treated for 1 h with CsA and then for 24 h with AA or control vehicle. RNA was isolated, and GLI1 mRNA expression was quantified by q-PCR. *Bars* and *error bars* represent means and S.E., respectively.

and lowered GLI1 expression (Fig. 6*C*). Finally, CsA treatment prevented the repression of GLI1 transcription by AA (Fig. 6*D*). These data suggest that a Ca^{2+}-calcineurin axis mediates the suppression of GLI1 expression by AA.

Because intracellular Ca^{2+} can be increased by reactive oxygen species, a common feature of cells treated with fatty acids, including AA (49–51), we examined the role of oxidative stress in the regulation of GLI1. As shown in Fig. 7*A*, the levels of hydroperoxides and activity of γ-glutamyl transpeptidase, two markers of oxidative stress, were elevated in PANC1 and MCF7 cells treated with AA. Treatment with antioxidants NAC and L-glutathione reversed the effect of AA on activation of CASP3 (Fig. 7*B*), GLI1 expression and promoter activity (Fig. 7, *C* and *D*), and nuclear translocation of NFATc1 (Fig. 7*D*, *right panel*). Taken together, these results indicated that *GLI1* is a novel target of the NFATc1 transcription factor, which acts as a mediator of the AA cytotoxic effect in cancer cells downstream of a reactive oxygen species-calcineurin axis.

AA Treatment Impairs Tumor Growth and Metastasis and Induces Apoptosis in Vivo—Next we defined the biological significance of the above findings by testing the ability of AA to inhibit tumor growth *in vivo* using a syngeneic mouse mammary tumor model (31). A significant reduction in tumor volume was observed in animals injected with AA every 7 days in the tumor bed compared with the control group ($p < 0.05$) (212.13 ± 13.4 *versus* 507.83 ± 139.06 mm^3) at 21 days post-treatment (Fig. 8*A*). Further analysis showed that AA reduced the number of lung metastases. Sections stained with H&E showed that mice treated with AA have a significantly lower incidence of lung metastases. Although metastases were observed in 57.14% of saline-treated mice, AA treatment resulted in a significant reduction in the incidence of lung metastasis (11.11%) ($p < 0.05$) (Fig. 8*B*).

Characterization of this phenotype demonstrated an increase in apoptosis in AA-treated tumors. TUNEL staining of tumors treated with AA showed an increased number of apo-

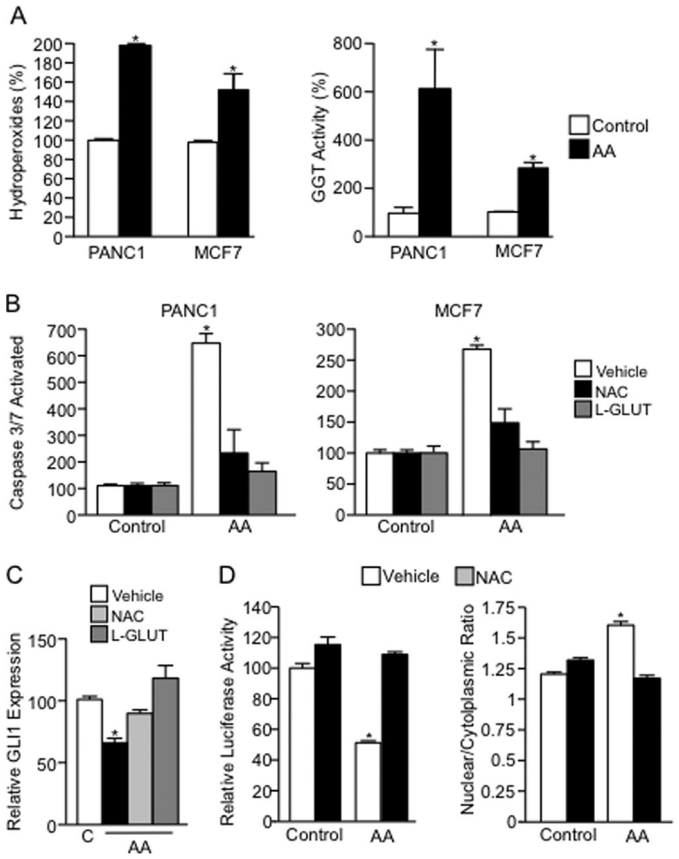

FIGURE 7. **Involvement of reactive oxygen species in AA effects on GLI1 expression.** *A*, hydroperoxides and γ-glutamyl transpeptidase (*GGT*) activity were measured in PANC1 and MCF7 cells treated ±AA. Activated CASP3/7 (*B*) and GLI1 mRNA expression (*C*) were measured in PANC1 and MCF7 cells pretreated with the antioxidants NAC and L-glutathione (*L-GLUT*) before treatment ±AA. *C*, control. *D*, transfected PANC1 cells were pretreated with NAC before treatment ±AA. *Left panel*, luciferase activity measured in cells transfected with the GLI1 promoter reporter shows that NAC abolishes the down-regulation of GLI1 promoter activity caused by AA. *Right panel*, measurement of the nuclear/cytoplasmic ratio of NFATc1 in cells transfected with NFATc1-GFP demonstrates that NAC prevents the AA-promoted increase in nuclear translocation of NFATc1. $n \geq 140$ cells per group. *, $p < 0.05$ *versus* the control group. *Bars* and *error bars* represent means and S.E., respectively.

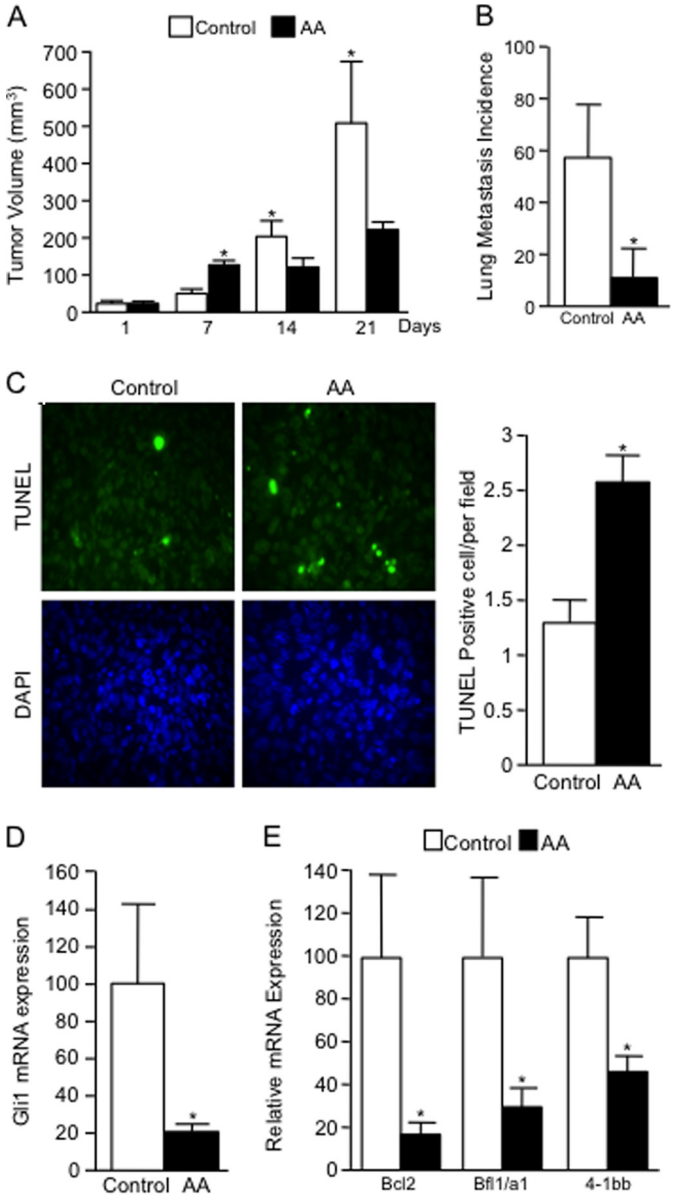

FIGURE 8. **AA treatment inhibits tumor growth and metastasis.** *A*, BALB/c mice were inoculated subcutaneously with 1×10^6 LM3 murine mammary adenocarcinoma cells. Tumor volume was measured in the mice treated ±AA every 7 days for 21 days. *Bars* and *error bars* represent means and S.E., respectively, calculated as follows: Tumor volume = Length × Width²/2. AA group, $n = 10$; control group, $n = 7$. *, $p < 0.05$ *versus* control group. *B*, lung tissues sections stained with H&E were analyzed for detection of metastasis. *C*, apoptosis evaluation in LM3 tumor section tissues by TUNEL assay (FITC labeling). TUNEL-positive cells in the nucleus are stained in *green*, and total nuclei are stained with DAPI in *blue* (at *left*). Data at *right* show *bars* and *error bars* representing means and S.E., respectively, for quantification of the apoptosis rates (average number of TUNEL-positive cells (stained in *green*) per visual field). Experiments were repeated in five tumor tissue sections for each condition. Ten fields of each section were selected at random for counting in a blinded manner; $n = 5$. *, $p < 0.05$ *versus* control group. *D* and *E*, relative mRNA levels determined by quantitative PCR for Gli1 (*D*) and Bcl2, Bfl1/a1, and 4-1bb (*E*) in tumors from control and AA-treated animals. *Bars* and *error bars* represent means and S.E., respectively; $n = 5$. *, $p < 0.05$ *versus* control group.

ptotic cells compared with control-treated mice (Fig. 8*C*). To confirm the effect of AA on the gene expression *in vivo*, we determined the expression of GLI1 and the antiapoptotic genes in LM3 tumors treated with or without AA. AA significantly decreased the mRNA expression of Gli1 (Fig. 8*D*) and Bcl2, Bfl1/a1, and 4-1bb genes (Fig. 8*E*) in LM3 tumors ($n = 5$).

Next, we examined whether pharmacologic inhibition of GLI1 using GANT61 (52) would mimic the effect of AA in LM3 cells *in vitro* and *in vivo*. Indeed, treatment of these cells with this inhibitor decreased cell viability and expression of Bcl2, Bfl1/a1, and 4-1bb genes (Fig. 9*A*) as well as tumor growth (Fig. 9*B*). Taken together, these data support a role for AA as an anticancer agent by affecting cell growth and inducing apoptosis *in vivo* and *in vitro*.

Discussion

PUFAs can regulate cellular behavior in all stages of carcinogenesis by acting as cytotoxic compounds, although in some cases these lipids promote tumor growth (20, 53–60). Our data show that the PUFA AA treatment impairs tumor volume *in vivo* and induces cell death *in vivo* and *in vitro*. Moreover, AA treatment decreases tumor progression as demonstrated by the lower number of lung metastasis. Consistent with the results presented here, local injection of the ω-6 PUFA γ-linolenic acid into a glioma tumor in a rat model has been shown to lead to

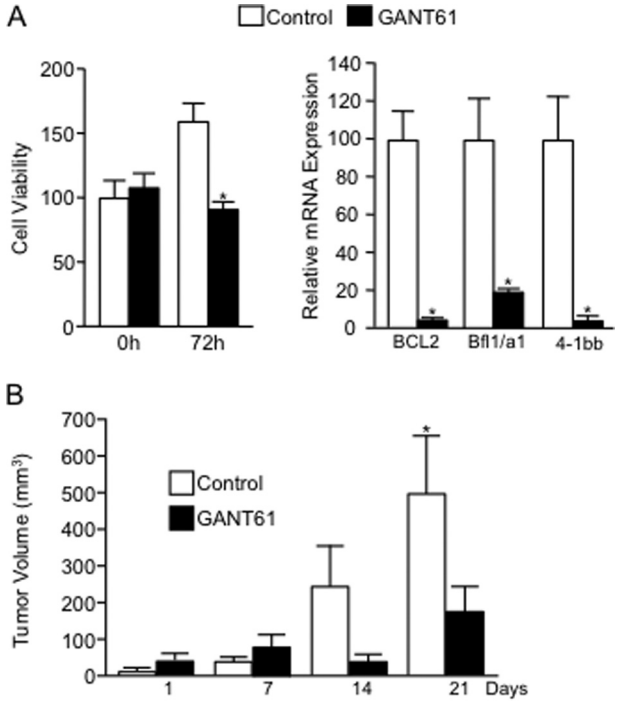

FIGURE 9. **Pharmacologic inhibition of GLI1 reduces tumor cell growth.** *A*, LM3 tumor cells were treated with GANT61 at s concentration of 20 μM for 72 h. Cell viability was then measured using resazurin (*left panel*), and antiapoptotic gene expression was measured by q-PCR. *, $p < 0.05$ *versus* control group. *B*, mice implanted with LM3 cells were treated with GANT61 (50 mg/kg), and tumor size was measured as in Fig. 8. *, $p < 0.01$ *versus* control group. *Bars* and *error bars* represent means and S.E., respectively.

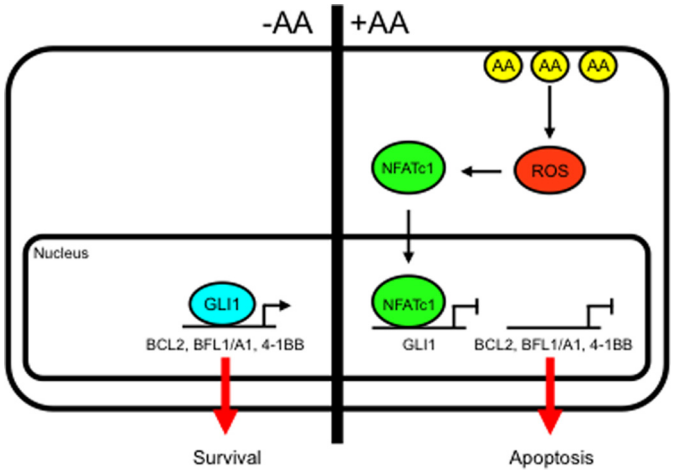

FIGURE 10. **Diagram of the proposed mechanism of AA-induced antitumoral activity.** This mechanism includes the NFATc1-dependent down-regulation of GLI1 and its target genes (*BCL2*, *BFL1/A1*, and *4-1BB*). *ROS*, reactive oxygen species.

tumor regression (8, 9). In addition, clinical studies show that intracerebral injection of γ-linolenic acid in patients with gliomas induces decreased tumor size (12, 13). Moreover, earlier studies had also shown that injection of LA and α-linolenic acid increases survival of rats with Mat 1376 ascites tumors (11). Subsequently, other studies showed that systemic treatment with the ω-6 PUFA LA decreased tumor growth and the incidence of metastases in a mouse model of lymphoma EL4 (10). Other reports have shown that AA has cytotoxic action, decreasing viability and inducing apoptosis in drug-resistant cancer cells (23–25, 56). Moreover, similar to our data, AA-enriched human colon cancer cells exhibited diminished cell viability and increased CASP-dependent apoptosis (20, 59). Although no studies have previously demonstrated a direct cytotoxic effect of AA on tumor development *in vivo*, it has been shown that, when intravenously infused, different radiolabeled PUFAs such as AA and docosahexaenoic acid induce rapid changes in the serum oxidant and antioxidant status, suggesting a possible therapeutic application in cancer (61, 62).

Our study elucidates a novel mechanism for AA as a cytotoxic lipid in cancer cells. We define a new signaling pathway induced by AA leading to a decrease in cell viability and increase in cell death by reducing the expression of a subset of antiapoptotic genes, BCL2, BFL1/A1, and 4-1BB. We showed that AA reduces the expression of these genes by regulating their promoter activity in a transcriptional manner. Several studies have demonstrated that AA reduces the expression of apoptosis-related proteins, including the known antiapoptotic protein BCL2 (20, 63, 64). However, no studies have linked AA or other PUFAs to the antiapoptotic genes BFL1/A1 and 4-1BB. In addition, our results establish for the first time a transcriptional mechanism that explains the cytotoxic antitumoral effects of AA in which the reduced transcription of these antiapoptotic genes is related to the down-regulation of the transcription factor GLI1.

We propose a new GLI1 regulatory mechanism that is independent of known cascades regulating the activity and expression of this transcription factor (65–67). Our data show that NFATc1 acts as a repressor by binding to the promoter of the *GLI1* gene in cells treated with AA. We further demonstrate that repression of GLI1 expression by NFATc1 in AA-treated cells is inhibited by antioxidants, suggesting that GLI1 repression by NFATc1 requires reactive oxygen species (Fig. 10). This conclusion is supported by the increase in reactive oxygen species detected in cells treated with AA (Fig. 6*A* and Refs. 17, 49, and 51). We also show that GLI1 repression by AA is blocked by CsA, an inhibitor of calcineurin. This result suggests that calcineurin plays a role in the signal cascade initiated by AA treatment in our studies, which is consistent with the known role of calcineurin in the activation of NFATc1 (46, 47). However, further studies are needed to determine the precise mechanisms of NFATc1 activation by AA. NFATc1 was first described as a regulator of T lymphocyte activation and differentiation and was subsequently implicated in the control of critical processes in many vertebrate systems (68, 69). NFATc1 has been reported to form nuclear complexes with different transcription factors (Stat3, NFκB, and CCAAT/enhancer-binding protein), thus activating the expression of genes that promote cell transformation and tumorigenesis (70–73). Nevertheless, recent studies indicate that NFAT complexes also can induce gene silencing via cooperation of transcription repressor proteins and members of the histone deacetylase family (74–76). NFATc1 complexes might similarly repress GLI1 expression by altering histone acetylation associated with the *GLI1* promoter.

Taken together, the results of this work show that natural nutrients such as PUFAs control the expression of target genes involved in carcinogenesis. Knowledge of the mechanisms by

which these PUFAs control specific gene expression may provide insight into the development of new therapeutic strategies and target drugs for anticancer treatment.

Author Contributions—A. C., L. L. A., E. J. T., E. I., D. L. M., M. G. F.-B., M. E. P., and M. E. F.-Z. conceived and coordinated the study and wrote the paper. A. C. designed, performed, and analyzed the experiments shown in Figs. 1–7 and 9. L. L. A., M. G. F.-B., and D. L. M. designed, performed, and analyzed the experiments shown in Figs. 2 and 4–7. A. L. V. designed and constructed vectors for expression and promoter studies. E. E.-H. designed, performed, and analyzed the experiments shown in Fig. 2. E. J. T. and E. I. designed, performed, and analyzed the experiments shown in Figs. 2 and 4. M. V. M., R. S., B. B., L. D. M., V. E., and A. R. E. provided technical assistance, essential reagents and contributed to the preparation of the figures. All authors reviewed the results and approved the final version of the manuscript.

Acknowledgments—We thank Emily Porcher for secretarial assistance and Gina Mazzudulli for technical assistance with the histological preparation.

References

1. Dahm, C. C., Gorst-Rasmussen, A., Crowe, F. L., Roswall, N., Tjønneland, A., Drogan, D., Boeing, H., Teucher, B., Kaaks, R., Adarakis, G., Zylis, D., Trichopoulou, A., Fedirko, V., Chajes, V., Jenab, M., Palli, D., Pala, V., Tumino, R., Ricceri, F., van Kranen, H., Bueno-de-Mesquita, H. B., Quirós, J. R., Sánchez, M. J., Luján-Barroso, L., Larrañaga, N., Chirlaque, M. D., Ardanaz, E., Johansson, M., Stattin, P., Khaw, K. T., Wareham, N., Wark, P. A., Norat, T., Riboli, E., Key, T. J., and Overvad, K. (2012) Fatty acid patterns and risk of prostate cancer in a case-control study nested within the European Prospective Investigation into Cancer and Nutrition. *Am. J. Clin. Nutr.* **96,** 1354–1361
2. Eynard, A. R., and Navarro, A. (2013) Crosstalk among dietary polyunsaturated fatty acids, urolithiasis, chronic inflammation, and urinary tract tumor risk. *Nutrition* **29,** 930–938
3. Tapiero, H., Ba, G. N., Couvreur, P., and Tew, K. D. (2002) Polyunsaturated fatty acids (PUFA) and eicosanoids in human health and pathologies. *Biomed. Pharmacother.* **56,** 215–222
4. Azrad, M., Turgeon, C., and Demark-Wahnefried, W. (2013) Current evidence linking polyunsaturated fatty acids with cancer risk and progression. *Front. Oncol.* **3,** 224
5. de Lorgeril, M., and Salen, P. (2012) New insights into the health effects of dietary saturated and ω-6 and ω-3 polyunsaturated fatty acids. *BMC Med.* **10,** 50
6. Wang, W., Zhu, J., Lyu, F., Panigrahy, D., Ferrara, K. W., Hammock, B., and Zhang, G. (2014) ω-3 polyunsaturated fatty acids-derived lipid metabolites on angiogenesis, inflammation and cancer. *Prostaglandins Other Lipid Mediat.* **113–115,** 13–20
7. Shaikh, I. A., Brown, I., Wahle, K. W., and Heys, S. D. (2010) Enhancing cytotoxic therapies for breast and prostate cancers with polyunsaturated fatty acids. *Nutr. Cancer* **62,** 284–296
8. Leaver, H. A., Wharton, S. B., Bell, H. S., Leaver-Yap, I. M., and Whittle, I. R. (2002) Highly unsaturated fatty acid induced tumour regression in glioma pharmacodynamics and bioavailability of gamma linolenic acid in an implantation glioma model: effects on tumour biomass, apoptosis and neuronal tissue histology. *Prostaglandins Leukot. Essent. Fatty Acids* **67,** 283–292
9. Miyake, J. A., Benadiba, M., and Colquhoun, A. (2009) Gamma-linolenic acid inhibits both tumour cell cycle progression and angiogenesis in the orthotopic C6 glioma model through changes in VEGF, Flt1, ERK1/2, MMP2, cyclin D1, pRb, p53 and p27 protein expression. *Lipids Health Dis.* **8,** 8
10. Salem, M. L. (2005) Systemic treatment with n-6 polyunsaturated fatty acids attenuates EL4 thymoma growth and metastasis through enhancing specific and non-specific anti-tumor cytolytic activities and production of TH1 cytokines. *Int. Immunopharmacol.* **5,** 947–960
11. Siegel, I., Liu, T. L., Yaghoubzadeh, E., Keskey, T. S., and Gleicher, N. (1987) Cytotoxic effects of free fatty acids on ascites tumor cells. *J. Natl. Cancer Inst.* **78,** 271–277
12. Bakshi, A., Mukherjee, D., Bakshi, A., Banerji, A. K., and Das, U. N. (2003) γ-Linolenic acid therapy of human gliomas. *Nutrition* **19,** 305–309
13. Das, U. N., Prasad, V. V., and Reddy, D. R. (1995) Local application of γ-linolenic acid in the treatment of human gliomas. *Cancer Lett.* **94,** 147–155
14. Bocca, C., Bozzo, F., Martinasso, G., Canuto, R. A., and Miglietta, A. (2008) Involvement of PPARα in the growth inhibitory effect of arachidonic acid on breast cancer cells. *Br. J. Nutr.* **100,** 739–750
15. Fukui, M., Kang, K. S., Okada, K., and Zhu, B. T. (2013) EPA, an ω-3 fatty acid, induces apoptosis in human pancreatic cancer cells: role of ROS accumulation, caspase-8 activation, and autophagy induction. *J. Cell. Biochem.* **114,** 192–203
16. Arita, K., Kobuchi, H., Utsumi, T., Takehara, Y., Akiyama, J., Horton, A. A., and Utsumi, K. (2001) Mechanism of apoptosis in HL-60 cells induced by n-3 and n-6 polyunsaturated fatty acids. *Biochem. Pharmacol.* **62,** 821–828
17. Dai, J., Shen, J., Pan, W., Shen, S., and Das, U. N. (2013) Effects of polyunsaturated fatty acids on the growth of gastric cancer cells *in vitro*. *Lipids Health Dis.* **12,** 71
18. Fenton, J. I., Hord, N. G., Ghosh, S., and Gurzell, E. A. (2013) Immunomodulation by dietary long chain ω-3 fatty acids and the potential for adverse health outcomes. *Prostaglandins Leukot. Essent. Fatty Acids* **89,** 379–390
19. Gleissman, H., Johnsen, J. I., and Kogner, P. (2010) ω-3 fatty acids in cancer, the protectors of good and the killers of evil? *Exp. Cell Res.* **316,** 1365–1373
20. Monjazeb, A. M., High, K. P., Connoy, A., Hart, L. S., Koumenis, C., and Chilton, F. H. (2006) Arachidonic acid-induced gene expression in colon cancer cells. *Carcinogenesis* **27,** 1950–1960
21. Sandrone, S. S., Repossi, G., Candolfi, M., and Eynard, A. R. (2014) Polyunsaturated fatty acids and gliomas: a critical review of experimental, clinical, and epidemiologic data. *Nutrition* **30,** 1104–1109
22. Yin, H., Zhou, Y., Zhu, M., Hou, S., Li, Z., Zhong, H., Lu, J., Meng, T., Wang, J., Xia, L., Xu, Y., and Wu, Y. (2013) Role of mitochondria in programmed cell death mediated by arachidonic acid-derived eicosanoids. *Mitochondrion* **13,** 209–224
23. Das, U. N., and Madhavi, N. (2011) Effect of polyunsaturated fatty acids on drug-sensitive and resistant tumor cells *in vitro*. *Lipids Health Dis* **10,** 159
24. Dymkowska, D., and Wojtczak, L. (2009) Arachidonic acid-induced apoptosis in rat hepatoma AS-30D cells is mediated by reactive oxygen species. *Acta Biochim. Pol.* **56,** 711–715
25. Falconer, J. S., Ross, J. A., Fearon, K. C., Hawkins, R. A., O'Riordain, M. G., and Carter, D. C. (1994) Effect of eicosapentaenoic acid and other fatty acids on the growth *in vitro* of human pancreatic cancer cell lines. *Br. J. Cancer* **69,** 826–832
26. Ruiz i Altaba, A., Mas, C., and Stecca, B. (2007) The Gli code: an information nexus regulating cell fate, stemness and cancer. *Trends Cell Biol.* **17,** 438–447
27. Kasper, M., Regl, G., Frischauf, A. M., and Aberger, F. (2006) GLI transcription factors: mediators of oncogenic Hedgehog signalling. *Eur. J. Cancer* **42,** 437–445
28. Mills, L. D., Zhang, Y., Marler, R. J., Herreros-Villanueva, M., Zhang, L., Almada, L. L., Couch, F., Wetmore, C., Pasca di Magliano, M., and Fernandez-Zapico, M. E. (2013) Loss of the transcription factor GLI1 identifies a signaling network in the tumor microenvironment mediating KRAS oncogene-induced transformation. *J. Biol. Chem.* **288,** 11786–11794
29. Nolan-Stevaux, O., Lau, J., Truitt, M. L., Chu, G. C., Hebrok, M., Fernández-Zapico, M. E., and Hanahan, D. (2009) GLI1 is regulated through Smoothened-independent mechanisms in neoplastic pancreatic ducts and mediates PDAC cell survival and transformation. *Genes Dev.* **23,** 24–36
30. Soria, E. A., Eynard, A. R., Quiroga, P. L., and Bongiovanni, G. A. (2007)

Differential effects of quercetin and silymarin on arsenite-induced cytotoxicity in two human breast adenocarcinoma cell lines. *Life Sci.* **81,** 1397–1402
31. Urtreger, A., Ladeda, V., Puricelli, L., Rivelli, A., Vidal, M., Delustig, E., and Joffe, E. (1997) Modulation of fibronectin expression and proteolytic activity associated with the invasive and metastatic phenotype in two new murine mammary tumor cell lines. *Int. J. Oncol.* **11,** 489–496
32. Zermati, Y., Mouhamad, S., Stergiou, L., Besse, B., Galluzzi, L., Boehrer, S., Pauleau, A. L., Rosselli, F., D'Amelio, M., Amendola, R., Castedo, M., Hengartner, M., Soria, J. C., Cecconi, F., and Kroemer, G. (2007) Nonapoptotic role for Apaf-1 in the DNA damage checkpoint. *Mol. Cell* **28,** 624–637
33. Elsawa, S. F., Almada, L. L., Ziesmer, S. C., Novak, A. J., Witzig, T. E., Ansell, S. M., and Fernandez-Zapico, M. E. (2011) GLI2 transcription factor mediates cytokine cross-talk in the tumor microenvironment. *J. Biol. Chem.* **286,** 21524–21534
34. Köenig, A., Linhart, T., Schlengemann, K., Reutlinger, K., Wegele, J., Adler, G., Singh, G., Hofmann, L., Kunsch, S., Büch, T., Schäfer, E., Gress, T. M., Fernandez-Zapico, M. E., and Ellenrieder, V. (2010) NFAT-induced histone acetylation relay switch promotes c-Myc-dependent growth in pancreatic cancer cells. *Gastroenterology* **138,** 1189–99.e1–2
35. Nye, M. D., Almada, L. L., Fernandez-Barrena, M. G., Marks, D. L., Elsawa, S. F., Vrabel, A., Tolosa, E. J., Ellenrieder, V., and Fernandez-Zapico, M. E. (2014) The transcription factor GLI1 interacts with SMAD proteins to modulate transforming growth factor β-induced gene expression in a p300/CREB-binding protein-associated factor (PCAF)-dependent manner. *J. Biol. Chem.* **289,** 15495–15506
36. Lo Ré, A. E., Fernández-Barrena, M. G., Almada, L. L., Mills, L. D., Elsawa, S. F., Lund, G., Ropolo, A., Molejon, M. I., Vaccaro, M. I., and Fernandez-Zapico, M. E. (2012) A novel AKT1-GLI3-VMP1 pathway mediates KRAS-induced autophagy in cancer cells. *J. Biol. Chem.* **287,** 25325–25334
37. Foy, K. C., Miller, M. J., Moldovan, N., Bozanovic, T., Carson, W. E., 3rd, and Kaumaya, P. T. (2012) Immunotherapy with HER-2 and VEGF peptide mimics plus metronomic paclitaxel causes superior antineoplastic effects in transplantable and transgenic mouse models of human breast cancer. *Oncoimmunology* **1,** 1004–1016
38. Yang, X., Cao, D., Wang, N., Sun, L., Li, L., Nie, S., Wu, Q., Liu, X., Yi, C., and Gong, C. (2014) *In vitro* and *in vivo* safety evaluation of biodegradable self-assembled monomethyl poly(ethylene glycol)-poly(ϵ-caprolactone)-poly(trimethylene carbonate) micelles. *J. Pharm. Sci.* **103,** 305–313
39. Hicks, M., and Gebicki, J. M. (1979) A spectrophotometric method for the determination of lipid hydroperoxides. *Anal. Biochem.* **99,** 249–253
40. Gardell, S. J., and Tate, S. S. (1983) Effects of bile acids and their glycine conjugates on γ-glutamyl transpeptidase. *J. Biol. Chem.* **258,** 6198–6201
41. Basso, M. M., Eynard, A. R., and Valentich, M. A. (2006) Dietary lipids modulate fatty acid composition, gamma glutamyltranspeptidase and lipid peroxidation levels of the epididymis tissue in mice. *Anim. Reprod. Sci.* **92,** 364–372
42. Biswas, D., Milne, T. A., Basrur, V., Kim, J., Elenitoba-Johnson, K. S., Allis, C. D., and Roeder, R. G. (2011) Function of leukemogenic mixed lineage leukemia 1 (MLL) fusion proteins through distinct partner protein complexes. *Proc. Natl. Acad. Sci. U.S.A.* **108,** 15751–15756
43. Senft, D., Berking, C., Graf, S. A., Kammerbauer, C., Ruzicka, T., and Besch, R. (2012) Selective induction of cell death in melanoma cell lines through targeting of Mcl-1 and A1. *PLoS One* **7,** e30821
44. Lavrrar, J. L., and Farnham, P. J. (2004) The use of transient chromatin immunoprecipitation assays to test models for E2F1-specific transcriptional activation. *J. Biol. Chem.* **279,** 46343–46349
45. Bigelow, R. L., Chari, N. S., Unden, A. B., Spurgers, K. B., Lee, S., Roop, D. R., Toftgard, R., and McDonnell, T. J. (2004) Transcriptional regulation of *bcl-2* mediated by the sonic hedgehog signaling pathway through gli-1. *J. Biol. Chem.* **279,** 1197–1205
46. Beals, C. R., Clipstone, N. A., Ho, S. N., and Crabtree, G. R. (1997) Nuclear localization of NF-ATc by a calcineurin-dependent, cyclosporin-sensitive intramolecular interaction. *Genes Dev.* **11,** 824–834
47. Medyouf, H., and Ghysdael, J. (2008) The calcineurin/NFAT signaling pathway: a novel therapeutic target in leukemia and solid tumors. *Cell Cycle* **7,** 297–303
48. Gurda, G. T., Guo, L., Lee, S. H., Molkentin, J. D., and Williams, J. A. (2008) Cholecystokinin activates pancreatic calcineurin-NFAT signaling *in vitro* and *in vivo*. *Mol. Biol. Cell* **19,** 198–206
49. Liu, W. H., and Chang, L. S. (2009) Arachidonic acid induces Fas and FasL upregulation in human leukemia U937 cells via Ca^{2+}/ROS-mediated suppression of ERK/c-Fos pathway and activation of p38 MAPK/ATF-2 pathway. *Toxicol. Lett.* **191,** 140–148
50. Prasad, A., Bloom, M. S., and Carpenter, D. O. (2010) Role of calcium and ROS in cell death induced by polyunsaturated fatty acids in murine thymocytes. *J. Cell. Physiol.* **225,** 829–836
51. Schönfeld, P., Schlüter, T., Fischer, K. D., and Reiser, G. (2011) Non-esterified polyunsaturated fatty acids distinctly modulate the mitochondrial and cellular ROS production in normoxia and hypoxia. *J. Neurochem.* **118,** 69–78
52. Lauth, M., Bergström, A., Shimokawa, T., and Toftgård, R. (2007) Inhibition of GLI-mediated transcription and tumor cell growth by small-molecule antagonists. *Proc. Natl. Acad. Sci. U.S.A.* **104,** 8455–8460
53. Comba, A., Lin, Y. H., Eynard, A. R., Valentich, M. A., Fernandez-Zapico, M. E., and Pasqualini, M. E. (2011) Basic aspects of tumor cell fatty acid-regulated signaling and transcription factors. *Cancer Metastasis Rev* **30,** 325–342
54. Comba, A., and Pasqualini, M. E. (2009) Primers on molecular pathways—lipoxygenases: their role as an oncogenic pathway in pancreatic cancer. *Pancreatology* **9,** 724–728
55. Das, U. N. (2006) Essential fatty acids: biochemistry, physiology and pathology. *Biotechnol. J.* **1,** 420–439
56. Gong, P., and Cederbaum, A. I. (2006) Transcription factor Nrf2 protects HepG2 cells against CYP2E1 plus arachidonic acid-dependent toxicity. *J. Biol. Chem.* **281,** 14573–14579
57. Hammamieh, R., Sumaida, D., Zhang, X., Das, R., and Jett, M. (2007) Control of the growth of human breast cancer cells in culture by manipulation of arachidonate metabolism. *BMC Cancer* **7,** 138
58. Hughes-Fulford, M., Li, C. F., Boonyaratanakornkit, J., and Sayyah, S. (2006) Arachidonic acid activates phosphatidylinositol 3-kinase signaling and induces gene expression in prostate cancer. *Cancer Res.* **66,** 1427–1433
59. Oraldi, M., Trombetta, A., Biasi, F., Canuto, R. A., Maggiora, M., and Muzio, G. (2009) Decreased polyunsaturated fatty acid content contributes to increased survival in human colon cancer. *J. Oncol.* **2009,** 867915
60. Pasqualini, M. E., Berra, M. A., Yurawecz, M. P., Repossi, G., and Eynard, A. R. (2008) Dietary manipulation of precursor PUFAs modulates eicosanoid and endocannabinoid synthesis: a potential tool to control tumor development. *Curr. Nutr. Food Sci.* **4,** 161–175
61. Giamarellos-Bourboulis, E. J., Skiathitis, S., Dionysiou-Asteriou, A., Donta, I., Hatziantoniou, S., Demetzos, K., Papaioannou, G. T., Karatzas, G., and Giamarellou, H. (2002) Rapid alterations of serum oxidant and antioxidant status with the intravenous administration of n-6 polyunsaturated fatty acids. *Prostaglandins Leukot. Essent. Fatty Acids* **67,** 57–62
62. Nariai, T., Greig, N. H., DeGeorge, J. J., Genka, S., and Rapoport, S. I. (1993) Intravenously injected radiolabelled fatty acids image brain tumour phospholipids *in vivo*: differential uptakes of palmitate, arachidonate and docosahexaenoate. *Clin. Exp. Metastasis* **11,** 141–149
63. Faragó, N., Fehér, L. Z., Kitajka, K., Das, U. N., and Puskás, L. G. (2011) MicroRNA profile of polyunsaturated fatty acid treated glioma cells reveal apoptosis-specific expression changes. *Lipids Health Dis.* **10,** 173
64. Lu, J., Caplan, M. S., Li, D., and Jilling, T. (2008) Polyunsaturated fatty acids block platelet-activating factor-induced phosphatidylinositol 3 kinase/Akt-mediated apoptosis in intestinal epithelial cells. *Am. J. Physiol. Gastrointest. Liver Physiol.* **294,** G1181–G1190
65. Dennler, S., André, J., Alexaki, I., Li, A., Magnaldo, T., ten Dijke, P., Wang, X. J., Verrecchia, F., and Mauviel, A. (2007) Induction of sonic hedgehog mediators by transforming growth factor-β: Smad3-dependent activation of Gli2 and Gli1 expression *in vitro* and *in vivo*. *Cancer Res.* **67,** 6981–6986
66. Fernández-Zapico, M. E. (2008) Primers on molecular pathways GLI: more than just Hedgehog? *Pancreatology* **8,** 227–229
67. Lauth, M., and Toftgård, R. (2007) Non-canonical activation of GLI transcription factors: implications for targeted anti-cancer therapy. *Cell Cycle* **6,** 2458–2463
68. Horsley, V., and Pavlath, G. K. (2002) NFAT: ubiquitous regulator of cell

differentiation and adaptation. *J. Cell Biol.* **156,** 771–774
69. Pan, M. G., Xiong, Y., and Chen, F. (2013) NFAT gene family in inflammation and cancer. *Curr. Mol. Med.* **13,** 543–554
70. Baumgart, S., Chen, N. M., Siveke, J. T., König, A., Zhang, J. S., Singh, S. K., Wolf, E., Bartkuhn, M., Esposito, I., Heßmann, E., Reinecke, J., Nikorowitsch, J., Brunner, M., Singh, G., Fernandez-Zapico, M. E., Smyrk, T., Bamlet, W. R., Eilers, M., Neesse, A., Gress, T. M., Billadeau, D. D., Tuveson, D., Urrutia, R., and Ellenrieder, V. (2014) Inflammation-induced NFATc1-STAT3 transcription complex promotes pancreatic cancer initiation by KrasG12D. *Cancer Discov.* **4,** 688–701
71. Kundumani-Sridharan, V., Van Quyen, D., Subramani, J., Singh, N. K., Chin, Y. E., and Rao, G. N. (2012) Novel interactions between NFATc1 (nuclear factor of activated T cells c1) and STAT-3 (signal transducer and activator of transcription-3) mediate G protein-coupled receptor agonist, thrombin-induced biphasic expression of cyclin D1, with first phase influencing cell migration and second phase directing cell proliferation. *J. Biol. Chem.* **287,** 22463–22482
72. Liu, Q., Chen, Y., Auger-Messier, M., and Molkentin, J. D. (2012) Interaction between NFκB and NFAT coordinates cardiac hypertrophy and pathological remodeling. *Circ. Res.* **110,** 1077–1086
73. Oh, M., Dey, A., Gerard, R. D., Hill, J. A., and Rothermel, B. A. (2010) The CCAAT/enhancer binding protein β (C/EBPβ) cooperates with NFAT to control expression of the calcineurin regulatory protein RCAN1–4. *J. Biol. Chem.* **285,** 16623–16631
74. Baumgart, S., Glesel, E., Singh, G., Chen, N. M., Reutlinger, K., Zhang, J., Billadeau, D. D., Fernandez-Zapico, M. E., Gress, T. M., Singh, S. K., and Ellenrieder, V. (2012) Restricted heterochromatin formation links NFATc2 repressor activity with growth promotion in pancreatic cancer. *Gastroenterology* **142,** 388–98.e1–7
75. König, A., Fernandez-Zapico, M. E., and Ellenrieder, V. (2010) Primers on molecular pathways—the NFAT transcription pathway in pancreatic cancer. *Pancreatology* **10,** 416–422
76. Mancini, M., and Toker, A. (2009) NFAT proteins: emerging roles in cancer progression. *Nat. Rev. Cancer* **9,** 810–820

Nuclear Factor of Activated T Cells-dependent Down-regulation of the Transcription Factor Glioma-associated Protein 1 (GLI1) Underlies the Growth Inhibitory Properties of Arachidonic Acid

Andrea Comba, Luciana L. Almada, Ezequiel J. Tolosa, Eriko Iguchi, David L. Marks, Marianela Vara Messler, Renata Silva, Maite G. Fernandez-Barrena, Elisa Enriquez-Hesles, Anne L. Vrabel, Bruno Botta, Lucia Di Marcotulio, Volker Ellenrieder, Aldo R. Eynard, Maria E. Pasqualini and Martin E. Fernandez-Zapico

J. Biol. Chem. 2016, 291:1933-1947.
doi: 10.1074/jbc.M115.691972 originally published online November 24, 2015
